A role for Wnt-β-catenin signaling in positioning motor neurons along the ventral nerve cord in *C. elegans*

Justin Evans

Thesis submitted to the Faculty of Graduate and Postdoctoral Studies in partial fulfillment of the requirements for the
Master of Science degree in Neuroscience

Department of Neuroscience
Faculty of Medicine
University of Ottawa

ABSTRACT

During *C. elegans* embryogenesis, the DD, DA, and DB motor neurons arise from left and right lineages, move towards the midline and intercalate into a single tract to form the ventral nerve cord (VNC). Recently, the non-canonical Wnt-planar cell polarity was shown to regulate cell intercalation during VNC assembly. Disruption of this pathway causes DD neurons to shift anteriorly along the anterior-posterior (AP)-axis. Here, we investigated the role of the canonical Wnt-β-catenin pathway in positioning neurons in the VNC. Mutations in canonical Wnt pathway components, including *bar-1*/β-catenin and *pop-1*/TCF, cause the anterior displacement of DD2 towards DD1. In contrast, disruption of the β-catenin destruction complex gene *pry-1*/Axin results in the posterior displacement of DD1 towards DD2. In order to determine where and when defects occur, we used fluorescent time-lapse imaging to follow DD, DA and RIG neuroblasts during embryogenesis. In wild-type, we found that RIGL and DA2 intercalate between DD1 and DD2 via T1-type cell neighbor exchanges. Dorsal-ventral (DV) constriction of the DD1 and DD2 cell junction results in these cells meeting at a central vertex, which then resolves when the RIGL and DA2 cell junction expands along the AP axis. The resolution of the central vertex results in the spatial displacement of DD1 and DD2 along the AP axis. However, in Wnt-β-catenin mutants, central vertex resolution defects result in decreased spacing between DD1 and DD2 that persist into adulthood.

TABLE OF CONTENTS

LIST OF FIGURES

LIST OF ABBREVIATIONS AND GENE NAMES

AP	anterior-to-posterior
APC	adenomatous polyposis coli
BAR-1	transcriptional β-catenin in *C. elegans*
C. elegans	*Caenorhabditis elegans*
CCC	cadherin-catenin complex
CE	convergent extension
CFZ-2	member of the Frizzled family
CKI	casein kinase I
CWN-1	member of the Wnt family
DA	Dorsal A neurons
DB	Dorsal B neurons
DD	Dorsal D neurons
DSH/DV	disheveled
DV	dorsal-ventral
EGL	egg laying defective
ELG-20	member of the Wnt family
FZ	frizzled
GSK3D	glycogen synthase kinase 3β
L(1,2,3,4)	larval stage
LEFT	lymphoid enhancer factor
LIN	lineage defective
LIN-17	member of the Frizzled family
LIN-18	member of the Ryk/Derailed family
LIN-44	member of the Wnt family
LRP6	low-density lipoprotein receptor-related protein 6
MIG	migration defective
MIG-1	member of the Frizzled family
MIG-5	member of the Frizzled family
ML	medial-lateral
MYO	myosin
N2	English *C. elegans* strain
NMY	non-muscle myosin
PCP	planar cell polarity
POP-1	sole TCF/LEF transcriptional member in *C. elegans*
PRY-1	member of the Axin family
RIG	head interneuron
SAX-3	ortholog of ROBO
TCF	T-cell factor
UNC	uncoordinated
VANG	Van Gogh
VNC	ventral nerve cord
WNT	combination of wg and int
WT	wild-type

ACKNOWLEDGMENTS

I first and foremost would like to thank my supervisor Dr. Antonio Colavita for his guidance and support throughout my project. He has been a supportive, encouraging, and thoughtful mentor. My research in Dr. Colavita's lab has challenged me to think critically, take on new challenges, and to learn how to be a better researcher; skills with which I take forward in my career.

I particularly would like to thank Jeffrey Huang, Tony Roenspies, and Nathaniel Noblett for their help during my time in Dr. Colavita's lab. I owe an enormous thanks to Tony for his countless hours teaching me molecular biology when I arrived in the lab, Jeffrey for showing me the microscopy ropes, and Nathaniel for helpful discussions and assistance. I would also like to thank Maerhyn Petite for her help in the lab.

I would like to thank my thesis advisory committee, Dr. Jonathan Lee and Dr. Woo Jae Kim, for their encouragement and feedback. To the welcoming UOttawa Brain and Mind Research Institute, including our lab neighbors in Dr. Michael Schlossmacher's lab.

Lastly, I would like to thank my friends and family. I would like to thank my parents Heather and Peter for cheering me on through my degree. To my partner Sarah, for her unconditional love and support. As well, to Rob and Alexandra, who's Sunday dinners have become an Ottawa staple.

CONTRIBUTION OF LAB MEMBERS

The design and direction of experiments were done under the supervision of Dr. Antonio Colavita. The contribution of lab members are as follows:

1. Jeffrey Hung, a previous MSc student in Dr. Colavita's lab, performed the initial candidate screen to showing that Wnt pathway components displayed DD1 and DD2 spacing defects. He also imaged the RIG neurons in Figures 7B-D.

2. Tony Roenspies, our lab technician, helped to image canonical Wnt-β-catenin mutants for DD position plots (used in Figure 5), generate PCR genomic fragments from the *bar-1* fosmid (used in Figure 8), and generate translational *bar-1* reporters (used in Figure 9, 10).

PART 1: INTRODUCTION

The formation of complex nervous systems in morphologically and functionally diverse organisms involves multiple biological processes. During development the patterning of cells, tissue architecture, and organs is tightly regulated. The Wnt signal transduction pathway is one of the major developmental signaling pathways that helps regulate these events.

Wnts are secreted lipid-modified glycoproteins that aid in the "developmental toolkit" of multicellular organisms. While the processes that utilize Wnts may differ, Wnts are highly conserved molecules with a common ancestor dating from the metazoan era nearly 650 million years ago (Rigo-Watermeier et al. 2012). The name Wnt was originally coined in the early 1980s by fusing the *Drosophila* polarity gene *wingless* (wg) with the vertebrate homolog *int-1* (Wodarz et al. 1998). Today there are now upwards of 100 Wnt genes that have been discovered in species ranging from complex vertebrates like humans and mice to relatively simple invertebrate species like the nematode *Caenorhabditis elegans (C. elegans)*.

1.1 Wnt ligands in C. elegans

While early metazoan ancestors had twelve Wnt genes (Janssen et al. 2010), the *C. elegans* genome contains only five Wnt genes (*cwn-1, cwn-2, egl-20, mom-2, lin-44).* This pruning of their ancestral repertoire has led *C. elegans* to rely less on combinatorial Wnt activity. A loss of MOM-2 causes 60% of embryos to die during development, whereas in *lin-44;cwn-1;cwn-2* or *lin-44;cwn-1;elg-20* triple mutants less than 5% embryos die (Gleason et al. 2006). Wnts are not only required for embryonic viability but also help regulate a diversity of biological processes.

Wnts can serve as both short- and long-range morphogens. In *Drosophila*, the formation of the wing imaginal disc utilizes a short and long Wnt signal. The short-range Wg signal is used to induce *achaete* gene expression, responsible for the striped pattern along the dorsal-ventral boundary, whereas long-range Wg signals target the wing development genes *vestigial* and *distalles* centered around the dorsal-ventral boundary (Zecca et al. 1996). Similarly, in *C. elegans* Wnts serve dual roles (Hardin et al. 2013). One short-range signaling event is involved in orienting the blastomere cells ABal, ABpr, ABpl, and Abar (or AB4s) during early embryogenesis. At the 8-cell stage, the blastomere C cell uses a contact-dependent Wnt signal to orient the AB4s, which was disrupted in *mom-2/Wnt* mutant. Thus, short-range MOM-2 may direct AB4 orientation (reviewed in (Walston et al. 2006)). Long-range Wnt signaling plays a prominent role in specifying the anterior-to-posterior (AP) axis. Each of the five Wnt ligands are expressed in a series of partially overlapping domains along the AP-axis: (anterior, head) *cwn-2*, *mom-2*, *cwn-1*, *elg-20*, and *lin-44* (posterior, tail)(Harterink et al. 2011). Therefore, cells undergoing long-range migrations can come into contact with distinct Wnt ligands. One example is the adoption of vulval cell fates in vulval precursor cells (VPCs). Inductive signals are required to ensure that VPCs do not fuse to the hypodermal syncytium. Of the five Wnt ligands, only CWN-1 and EGL-20, which are expressed posterior to the vulval, prevent inappropriate fusion of VPCs.

1.2 Wnt pathways overview

When Wnts are released their diffusion creates signal gradients. Therefore overlapping Wnts can transfer positional information to coordinate cell position. Neurons also employ

distinct strategies to regulate Wnt input through diverse receptors. In *C. elegans* there are five Frizzled (*lin-17*, *mom-5*, *mig-1*, *cfz-2*) receptors, and a single Ryk/Derailed (*lin-18*) and ROR receptor (*cam-1*). Together, the combination of diverse guidance cues and receptors aid in cell-specific processes. Cells also respond to Wnt signals through overlapping pathways including the canonical Wnt-β-catenin, Wnt-β-catenin asymmetry, and the non-canonical Wnt-planar cell polarity (PCP) pathway.

1.2.1 Canonical Wnt-β-catenin

Wnt ligands affect gene transcription through the intracellular signal transducer β-catenin. Free β-catenin is normally captured by the 'destruction' complex, consisting of the tumor suppressor protein APC, scaffolding protein Axin, and the kinases CKI and GSK3β, which targets it for proteasome-mediated degradation. However, binding of secreted Wnt ligands to Frizzled transmembrane receptors and the low-density lipoprotein receptor-related proteins LRP5 or LRP6, leads to phosphorylation of an LRP intracellular domain and recruitment of the destruction complex. Recruitment and inactivation of the destruction complex by its coreceptor results in a stable pool of soluble β-catenin. Free β-catenin enters the nucleus where it regulates gene expression through the transcription factor TCF/LEF (Figure 1)(Fagotto 2013).

The transport of Wnt-stabilized β-catenin into the nucleus to interact with its binding partner TCF/LEF remains unclear. As β-catenin does not have a classic nuclear localization signal (NLS) or nuclear export signal (NES) it has been proposed that APC, which has two NLS and five NES signals, assists in the transportation of β-catenin (reviewed in (Henderson et al. 2002)). APC and Axin have been shown to mediate nuclear export of β-catenin (Cong et al.

2004; Henderson 2000). Thus, APC and Axin regulation of β-catenin is two-fold, the degradation in the cytoplasm by the APC-axin destruction complex and nuclear export. Nuclear export of β-catenin is also regulated by the inner nuclear membrane protein emerin through a conserved APC-like binding domain (Markiewicz et al. 2006). However, β-catenin can enter and exit the nucleus independent of APC and other classic nuclear transport receptors (Wang et al. 2014; Wiechens et al. 2001). This supports a model where β-catenin can freely diffuse throughout the cell but is actively restricted or degraded to regulate its localization.

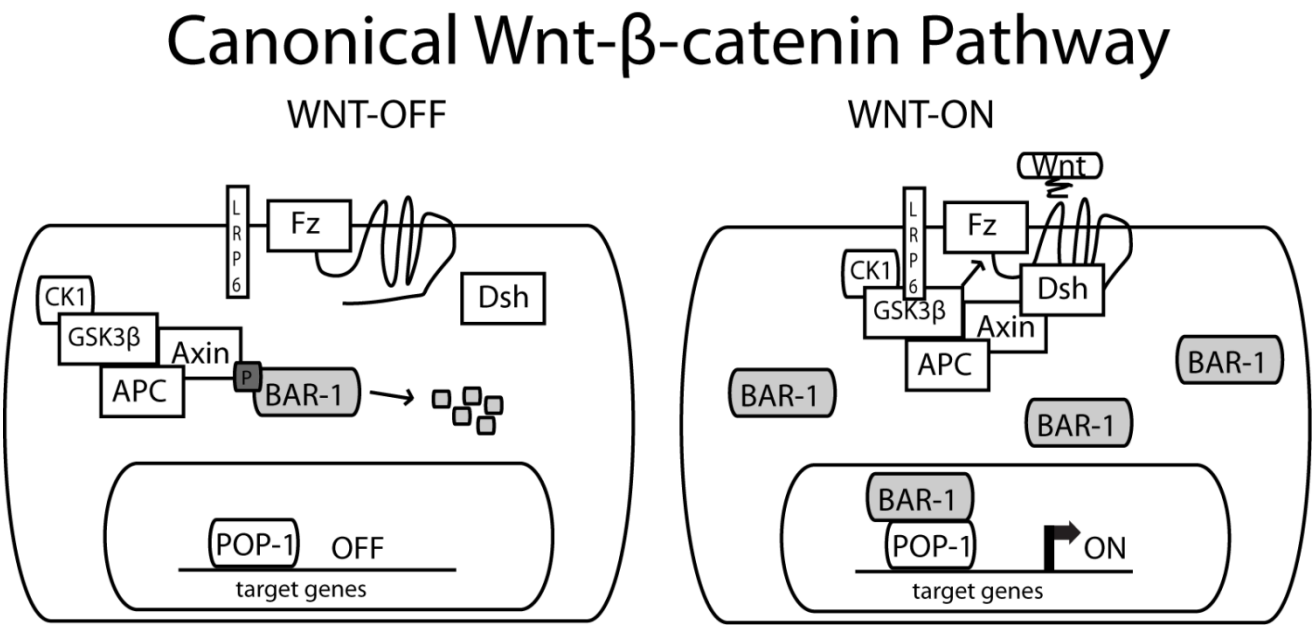

Figure 1. The Canonical Wnt-β-catenin Pathway in *C. elegans*
WNT-OFF: In *C. elegans* β-catenin (*bar-1*) is captured by the destruction complex and targeted for proteasome-mediated degradation. The destruction complex consists of APC (*apr-1*), Axin (*pry-1*), GSK3β (*gsk-3*), and CK1 (*kin-19*). WNT-ON: When Wnts (*cwn-1, cwn-2, egl-20, lin-44, mom-2*) binds to a transmembrane Frizzled receptors (*lin-17, mig-1, cfz-2, mom-5*) and LRP6, the destruction complex is recruited to the cell membrane and inactivated in a process involving the cytoplasmic protein Dishevelled (*mig-5, dsh-1, dsh-2*). Free β-catenin can then enter the nucleus and bind to its transcriptional TCF (*pop-1*) target.

1.2.2 Diversification of β-c*atenins and the cadherin-catenin complex*

β-catenins are classified based on their role in the cadherin-catenin complex (CCC) or their ability to regulate gene expression. The CCC helps regulate intercellular cell-cell adhesion through the indirect association of extracellular cadherins with the intracellular cytoskeleton. In vertebrates, cadherin-β-catenin interactions involve a p120 subfamily group, γ-catenin/plakoglobin, and three plakophilin proteins, whereas Wnt-mediated transcriptional activity is regulated by a single β-catenin (reviewed in (McCrea et al. 2010)). In invertebrates, there are fewer catenin proteins. In *Drosophila* a single β-catenin (Armadillo) regulates cell adhesion and Wnt signaling. However, in *C. elegans* there are four divergent β-catenin (BAR-1, SYS-1, WRM-1, HMP-2) and single α-catenin (HMP-1). While vertebrates Wnt-β-catenin signaling uses a single β-catenin and multiple TCF/LEF transcription factors to affect gene transcription (Hoppler et al. 2007), *C. elegans* use multiple β-catenins to regulate a single TCF/LEF factor (POP-1)(Jackson et al. 2012).

1.2.3 Wnt-β-catenin asymmetry

The asymmetric localization of cellular components during a cell division produces daughter cells that differ in cell fate. The localization of Wnt-β-catenin pathway components aid in the specification of anterior or posterior daughter cells. The primary role of β-catenin in Wnt-β-catenin asymmetry is to regulate the asymmetrical localization of POP-1/TCF. Activation of

WRM-1/β-catenin in posterior daughter cells phosphorylates the LIT-1/Nemo-like kinase, leading to a nuclear export of POP-1 by the polarity protein PAR-5 (Lo et al. 2004). Therefore, WRM-1 is preferentially enriched in the nucleus of posterior daughter cells and POP-1 is enriched in anterior daughter cells (Zacharias et al. 2015; Nishimura et al. 2012).

Additional β-catenins also function to regulate asymmetric cell division. SYS-1 is another divergent β-catenin (Liu et al. 2008) in *C. elegans*. While SYS-1/β-catenin is not required for POP-1 asymmetry (Siegfried et al. 2004), it acts as a coactivator of POP-1 (Huang et al. 2007). However, binding of POP-1 by either SYS-1 and WRM-1 is mutually exclusive (Yang et al. 2011). Thus, in the context of anterior-posterior cell asymmetry, SYS-1 binding to POP-1 activates Wnt target genes, whereas POP-1 binding in the absence of SYS-1 leads to repression (Yang et al. 2011; Murgan et al. 2015). Disruption of the SYS-1-to-POP-1 ratio in *C. elegans* leads to dysregulated AP fate decisions in seam cells (Lin et al. 1998), pharynx (Huang et al. 2007), and gonads (Siegfried et al. 2002).

1.2.4 The Non-canonical Wnt-planar cell polarity pathway

The 'non-canonical,' or Wnt-planar cell polarity pathway (PCP), is involved in the coordination of individual cell polarity and polarized tissues. Much like the canonical Wnt-β-catenin pathway, extracellular signals are transmitted through Frizzled-Dishevelled interactions, but diverge further downstream. Unique to the PCP pathway is the asymmetrical distribution of protein complexes. The main components of the PCP pathway are the membrane proteins Frizzled (Fz), Flamingo (Fmi) and Van Gogh (Vang) and the cytoplasmic proteins, Dishevelled

(Dsh) and Prickle (Pk) (Devenport 2016). The organization of these protein complexes helps regulate diverse morphogenic processes.

The core PCP pathway components were originally found in *Drosophila*. In the *Drosophila* wing system simple alignment of actin hairs (or trichomes) are polarized along the proximal and distal axes. However, in PCP mutants trichomes arise ectopically in the center of cells or exhibit improper alignment along the wing axis (Maung et al. 2011). The mechanism by which PCP signaling helps regulate polarized rearrangements involves the cytoskeleton. PCP signaling leads to the activation of conserved cytoskeletal regulators such as Rac and RhoA GTPases and the microtubule-associated protein c-Jun N-terminal kinase (JNK). A loss of Rho produced PCP defects similar to both Fz and Dsh mutants (David I. Strutt 1997). Subsequent studies showed that in addition to RhoA being a key regulator of myosin-II-mediated actin dynamics (Sai et al. 2014), Prickle can inhibit RhoA activity (Zhang et al. 2016). PCP components can also regulate each other. Diego can bind Dishevelled and promote Frizzled signaling whereas Prickle acts as a Frizzled antagonist (Jenny et al. 2005). Together this supports a model where the polarity and intercellular antagonism of specific PCP complexes like Fzd/Dvl and Vangl/Pk1 can regulate cytoskeleton rearrangements. The non-canonical Wnt-planar cell polarity pathway can also affect non-static cells.

1.3 Wnts in neuronal position

Wnts play an important role during nervous system development by regulating neuronal migration. Wnts regulate neuronal migration during embryogenesis (including the HSN, ALM, CAN, and BDU neurons) and larval development (QL/QR neurons)(Sawa H. 2013). Due to their

invariant cell lineages and relatively simple neuronal patterning, these neurons have led to an increased understanding of how Wnt guidance cues regulate neuronal position.

1.3.1 Embryonic Wnt signaling in neuronal migration

Both Wnt and their Frizzled receptors regulate the migration of the hermaphrodite-specific neurons (HSNs) during embryogenesis. These bilaterally symmetric motor neurons are generated in the tail of the embryo and migrate anteriorly towards the mid-body region. In *egl-20* mutants HSN exhibits a strong undermigration phenotype, whereas the loss of other Wnt ligands as seen in *cwn-1*, *cwn-2* or *mom-2* mutants do not exhibit strong defects. This suggests EGL-20 acts as a repulsive guidance cue for HSN migration. However, loss of other Wnt ligands in an *egl-20* mutant enhances migration defects, suggesting multiple Wnts cooperate to regulate HSN migration. Similarly, while only *mig-1*/Frizzled displayed an HSN migration defect, double mutants with either *mom-5*, *cfz-2*, and *lin-18*/Ryk enhanced the *mig-1* phenotype (Pan et al. 2006). Interestingly, CAM-1 affects HSN migration through an independent mechanism. CAM-1 is proposed to act as a 'sink' for EGL-20 by inhibiting its signaling activity during HSN migration. Therefore, overexpression of CAM-1 results in the posterior displacement of HSN (Kim et al. 2003), whereas *elg-20* and *cam-1* mutants exhibited an anterior phenotype (Forrester et al. 2004).

The canal-associated neurons (CANs) also utilize Wnt signaling components during migration. Both CAN and HSN migrate towards the mid-body region, despite starting from opposite ends in the head and tail, respectively (Silhankova et al. 2007). Just as in HSN migration, specific Wnt and Frizzled combinations affect CAN migration. Mutations in *cwn-2*

alone cause posterior defects, whereas mutations in *cwn-1* and *egl-20* do not. However, in double mutants *cwn-1* or *egl-20* enhanced *cwn-2*-dependent defects, suggesting these proteins cooperate to regulate CAN migration. Interestingly, loss of Frizzled proteins resulted in an anterior migration phenotypes, the opposite of what was observed in Wnt mutants. Disruption of both *cfz-2* and *mom-5*, but not *lin-17* and *mig-1*, lead to anterior CAN defects (Zinovyeva et al. 2008). CANs also utilize the ROR receptor tyrosine kinase CAM-1 (or CAN-Abnormal-Migration) to regulate EGL-20 repellent cues. CAM-1 expression in CANs appears to act as an extracellular Wnt-binding domain to dampen repulsive EGL-20 and CWN-1 signals (Modzelewska et al. 2013). Interestingly, this supports a model where CAM-1 expression from CANs sequesters EGL-20 ligands necessary for normal HSN migration.

1.3.2 Larval Wnt signaling in neuronal migration

The Q neuroblasts are a well-studied example of Wnt-mediated migration during larval development in *C. elegans*. The left Q neuroblast (QL) and right Q neuroblast (QR) are born at equivalent AP positions, yet exhibit opposite migratory behavior as a result of EGL-20 guidance cues (Harris et al. 1996). QL migrates posteriorly and QR migrates anteriorly. An EGL-20-dependent pathway regulates the expression of the Hox gene *mab-5* in QL and its descendants to direct them to migrate posteriorly. Thus in *egl-20* mutants, when *mab-5* is not expressed in QL, both QL and QR migrate anteriorly. The level of EGL-20 is also important for Q neuroblast migration. Overexpression of EGL-20 resulted in both descendants of QR and QL to migrate posteriorly by inducing *mab-5*-dependent migration. Whereas, low EGL-20 levels promoted the anterior migration of QR descendants and QL descendants to remain posterior. This suggests

high levels of EGL-20 activates a Wnt signaling pathway, whereas low levels activate migration through an independent pathway (Whangbo et al. 1999). Interestingly, a delay in the anterior migration of QL is observed in *mab-5* but not *egl-20* mutants, suggesting EGL-20 may acutely inhibit migration through MAB-5 independent mechanisms (Josephson et al. 2016). Taken together, studies of Q neuroblast migration highlight how neurons utilize Wnt signals to carry out diverse migration strategies.

1.3.3 The PCP pathway in cell migration

PCP components can influence cell migration. During migration cells extend polarized actin-rich cell feet, known as lamellipodia, which aid in the generation of cell movements. In *Drosophila*, a loss of PCP components leads to a reduction in actin-rich protrusions (Bastock et al. 2007). In *Xenopus* PCP components also direct cell migration through repulsive cues. In migrating neural crest cells, cell-cell contact results in PCP-dependent activation of RhoA and a loss of cell protrusions (Carmona-Fontaine et al. 2008; Aman et al. 2010). Thus, follower cells can direct the migration of leadings cells through RhoA-dependent repulsive activity. PCP signaling are also known to affects microtubule based cell protrusions known as cilia (Wallingford 2006). Ciliated cell that lack either PCP effectors proteins, Inturned and Fuzzy, fail to accumulate actin apically, accumulate elongated microtubules intracellularly, and can have abnormal oriented microtubules (Park et al. 2006). Together, these findings support a model in which PCP components can affect many cellular migration strategies.

1.4 Convergent extension

Convergent extension (CE) involves regulated cell intercalation movements that act to narrow tissues along one axis while elongating them along the perpendicular axis. In general, the CE of the body axis involves three phases: 'dorsal convergence,' which involves the directional migration of individual cells towards the midline; 'medial-lateral (ML) intercalation,' of cells at the dorsal midline; and 'anterior-to-posterior (AP)' extension of cells along the body axis (Wallingford et al. 2002). The combination of these collective cell movements requires cells to coordinate cellular rearrangements and tissue geometry.

Junctional rearrangements underlie changes in tissue geometry. At its core cells form and break bonds to permit changes in tissue connectivity. A cell neighbor exchange, simply defined as a pair of adjacent cells that attach to or separate from one another, underlie different types of junctional rearrangements. These types of junctional rearrangements include: a T1 transition, involving four cells, where constrictions along one cell junction forms a central vertex and resolves to create a new cell junction; a T2 transition, where cell area is removed, often as a result of apoptosis; a T3 transition, where an intercalating cell forms a new vertex that is then replaced with two new vertices; and a rosette, where five or more cells, meet at a central vertex (Figure 2)(reviewed in (Fletcher et al. 2014)). Diverse junctional rearrangements therefore underlie many CE processes.

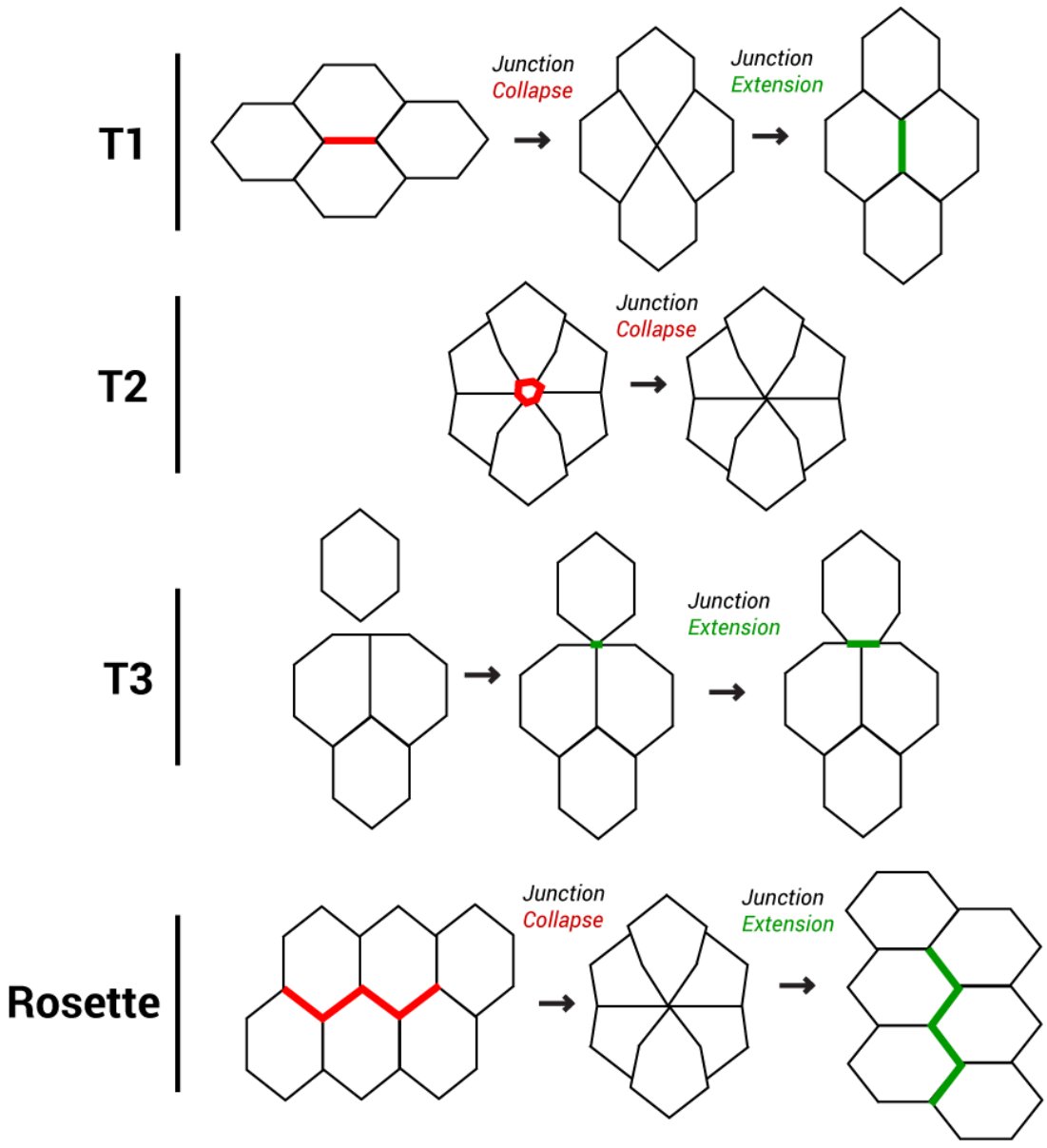

Figure 2. Summary junctional rearrangements
A series of junctional rearrangements where a collapse of junctions (red) and the creation of a new junction (green) are indicated. Summary of each event previously described (section 1.4). Reviewed in (Fletcher et al. 2014).

1.4.1 The PCP pathway in convergent extension

The first evidence that the PCP pathway was involved in regulating CE came from studies of *Xenopus* neurulation. During formation of the *Xenopus* neural tube, mesodermal cells extend lamellipodium, actin-rich cell feet, which protrude at random prior to gastrulation. Cellular protrusions are arranged along the medial and lateral sides of intercalating cells during convergence of the mesoderm. However, this protrusive activity is lost when cells reach their contacting boundary (reviewed in(Wallingford 2006; Wallingford et al. 2002)), which suggests cells tightly regulate polarization. In embryos that lacked the dishevelled homolog (Xdsh) cells did not polarize and did not undergo proper CE (Wallingford et al. 2000). Likewise, a loss of the Van Gogh homolog (Vang), which is expressed in anterior neural plate and posterior notochord, do not exhibit polarized protrusive activity during CE (Goto et al. 2002).

Since the initial findings in *Xenopus*, the PCP pathway has been shown to play a central role in CE-mediated neural tube development. Initial work found that mutations in the PCP component Van Gogh results in NTDs in both mice and humans (Torpe et al. 2014; Reynolds et al. 2007). Subsequent work found that mutations in either Frizzled or Flamingo lead to defects in vertebrate neurulation (Curtin et al. 2003; Yanshu Wang, Nino Guo 2006).

Recent work has sought to characterize the molecular mechanisms that underlie neural tube formation. During neural plate bending Dishevelled proteins aids in the recruitment of Rho kinase (ROCK). ROCK activates myosin II in order to organize contractive cables across the neural folds. The resulting contraction shortens the neural plate along its apical edge via individual cadherin-based adherens junctions (Nishimura et al. 2012).

1.4.2 Ventral nerve cord (VNC) assembly in C. elegans: a new CE model

At hatching the *C. elegans* ventral nerve cord consists of three classes of motor neurons (DD1-6, DA1-9, and DB1-7). Each motor neuron is stereotypically placed in a single-file line along the AP-axis. However, during embryogenesis these neurons arise from their respective left and right lineages and must undergo a convergent extension process to reach their final AP positions. After being born cell constriction along the medial-lateral (ML) axis drives the DAs and DDs together in an alternating sequence as they intercalate towards the midline. Upon meeting at the midline, ventral neuroblasts form a set of intermediary rosettes structures. Formation of these rosettes follows a temporal order, with the anterior most rosette forming first and the posterior rosette last. Following resolution, single cell intercalations lead the neuroblasts to form a single file along the embryonic VNC that remains through larval development (Figure 3).

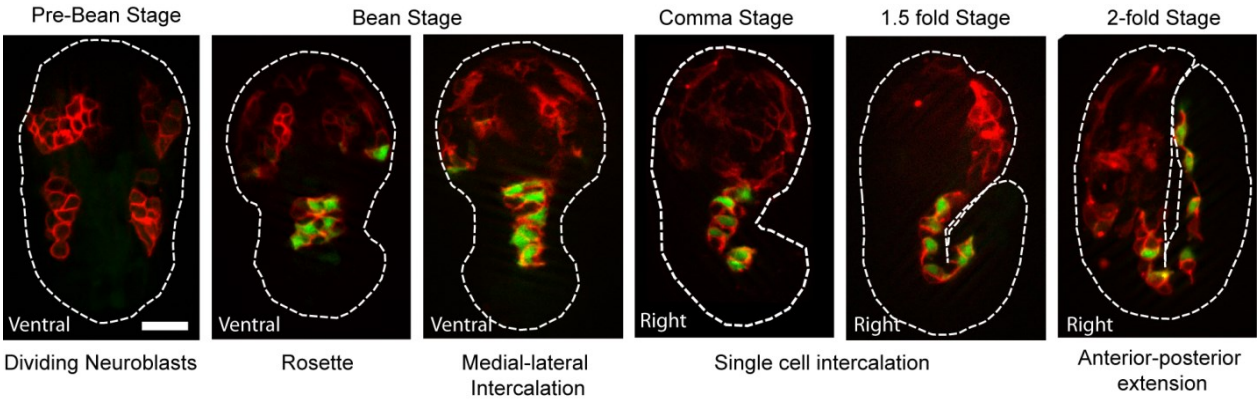

Figure 3. Convergent extension of the *C. elegans* ventral nerve cord
An overview of convergent extension (CE) of the ventral nerve cord (VNC). Embryos are in a *zyIs40*[*unc-30p::gfp cnd-1p::PH::mCherry]* background to visualize DA (mCherry) and DD (GFP and mCherry) neurons. At the pre-bean stage DA and DD neurons are born on either side of the embryo. Constrictions along the medial-lateral axis bring the neuroblasts together at the ventral midline. At the bean stage neuroblasts form a set of intermediary rosettes structures that resolve in strict temporal order. Single-celled intercalation at the comma stage results in neuroblasts forming a single file along the anterior-to-posterior axis. Anterior-to-posterior ordering of neuroblasts at the 2-fold stage remains through larval development.

Our lab has recently shown that cell intercalation-mediated VNC assembly involves the activities of the planar cell polarity and SAX-3/Robo pathways (Shah et al. 2017; Soto 2017). Whereas the six DD neurons (DD1-6) are evenly spaced along the AP-axis in wild-type, disruption of either of these pathways causes DD neurons to shift anteriorly. Double mutants with *sax-3* and either *vang-1* or *prkl-1* enhance DD neuron defects; suggesting that these two pathways act in parallel to regulate DD neuron spacing. Defects in DD neuron position arise due to a failure of proper CE during VNC assembly. In the embryo, PCP and sax-3 mutants exhibited delays in rosette-resolution of the ventral neuroblasts. PCP signaling has also been shown to coordinate multicellular rosettes in vertebrates (Trichas et al. 2012). Defects in PCP and *sax-3* mutants arose from a delay of rosette-resolution during embryogenesis. Delays in rosette resolution lead the DA and DD neurons to enter the presumptive VNC later in development, resulting in an anterior displacement of neuroblasts that persists through adulthood. In addition, protein localization of VANG-1, SAX-3, and NMY-2 (myosin II) was shown to be enriched at contracting cell contacts and rosette foci, consistent with the idea that these proteins regulate cell intercalation during VNC assembly. Together these findings set the stage for VNC assembly to be a relatively simple model to investigate new pathways involved in CE-based neural tube formation.

1.4.3 The Wnt-β-catenin pathway in convergent extension

While the role of the non-canonical Wnt/PCP signaling in CE and cell-intercalation is well known, the role of the canonical Wnt-β-catenin pathway in CE remains poorly understood.

In *Xenopus*, the canonical Wnt-β-catenin pathway has been shown to regulate CE during gastrulation. Disruption of Wnt-β-catenin signaling using LEF-1 mutants, which are unable to bind β-catenin, or embryos injected with the RNA conductin, which triggers β-catenin degradation, resulted in CE defects. The transcription factor *siamois* and TGF-*β* family member *Xnr-3,* both known Wnt-β-catenin target genes, were assessed for their ability to rescue Wnt-β-catenin defects. Interestingly, overexpression of *Xnr-3*, but not *siamois*, was able to rescue CE defects in LEF-1 mutants or conductin injected embryos (Kühl et al. 2001). These findings suggest that upstream Wnt-β-catenin components rather than Wnt-β-catenin-mediated control of gene expression regulate CE in *Xenopus* gastrulation. Independent work by Wallingford *et al.* 2001 also showed that co-expression of the dominant-negative GSK3, which aids in the phosphorylation of β-catenin for degradation, failed to rescue Xwnt5a/Wnt and Nxfz-8/Frizzled CE defects (Wallingford et al. 2001). This suggests CE-dependent defects in Wnt and Frizzled mutants are not a result from downregulating β-catenin in *Xenopus*.

At the receptor level, canonical and non-canonical Wnt-β-catenin activity interact during CE. In zebrafish, the receptor CD146 regulates cell motility, polarity, and CE during gastrulation through Wnt5a activation of non-canonical Wnt signaling. However, CD146 also promotes β-catenin degradation in the cytosol, which suggests the receptor is a negative regulator of canonical Wnt signaling (Ye et al. 2013). Similarly, in *Xenopus* the lipoprotein receptor-related protein 6 (LRP6) is known to regulate CE through the activation of PCP signaling. However, Lrp6 has also been shown to regulate CE by coordinating the switch from Wnt/PCP to Wnt-β-catenin activity (Tahinci et al. 2007). Although disrupting either CD146 or Lrp6 causes CE defects in their respective model, to what extend these receptors regulate CE through canonical Wnt-β-catenin activity alone is not understood.

1.5 Objectives

Objective: The role of the Wnt-β-catenin pathway in convergent extension remains poorly understood. Therefore, I will determine the role of Wnt-β-catenin signaling in ventral nerve cord assembly, the newly identified convergent extension model in *C. elegans*. I will therefore:

I. Conduct a candidate screen of canonical Wnt-β-catenin pathway components
II. Link embryonic ventral nerve cord defects in Wnt-β-catenin mutants to adult neuron position

PART 2: MATERIALS AND METHODS

2.1 C. elegans Strains

The *C. elegans* Bristol N2 strain was used as wild-type (*wt*). Worm strains were obtained from the *C. elegans* Genetic Center (University of Minnesota, Minneapolis), and cultured at either 20°C or 25°C. The following alleles were used: *lin-44(n1792), cwn-1(ok546), cwn-2(ok895), egl-20(n585), lin-17(n677), mig-1(n687), cfz-2(ok1445), mig-5(tm2639), bar-1(ga80), bar-1(mu350), pop-1(hu9),* and *pry-1(mu38).* Transgenes used include: *ynIs37*[*flp-13p::gfp*], *zyIs27*[*flp-13p*::*gfp*; *unc-129p*::*mCherry*; *myo-2p*::*mCherry*], *zyIs32[flp-13::gfp; flp-18::gfp], zyIs36*[*cnd-1p*::*PH*::*mCherry*; *myo-2p*::*mCherry*], and *zyIs40*[*unc-30p::gfp;cnd-1p::PH::mCherry;myo-2p*::*mCherry]*. Extrachromosomal transgenes: zyEx80[*bar-1p::bar-1::gfp*], zyEx(pan-neuronal)[*unc-33p::bar-1::gfp*], and zyEx(pan-epidermal)[*dpy-7::bar-1::gfp*]; *bar-1* genomic fragments: zyEx(short)[7.5kb *genomic fragment*], zyEx(medium)[10.1kb *genomic fragment*], zyEx(long)[11.7kb *genomic fragment*].

2.2 Molecular biology and transgenic lines

The 9.4kb BAR-1::GFP construct was made using overlap fusion PCR (Hobert 2002). The 5.1kb BAR-1 promotor (5'-gatctgttga… gcctaggtcc-3') was amplified from a bar-1p::bar-1cDNA plasmid (a gift from David Eisenmann, University of Maryland, Baltimore) and fused to a 4.3kb bar-1cDNA::GFP::unc-54UTR (5'-gatctgttga… atataaccct-5') fragment amplified from a unc-47p::bar-1cDNA::GFP::unc-54UTR containing transgenic strain (a gift from Kang Shen, Stanford University).

For tissue-specific rescue experiments, *unc-33* (pan-neuronal) and *dpy-7* (pan-epidermal) (Myers et al. 2007) promoters were used to drive *bar-1* expression. Constructs were made using overlap fusion PCR. The 2kb *unc-33* promoter (5'-tagcaagaag…ataactgttt-3') and 434bp *dpy-7* promoters (5'-gtgtgatcga…ttccagataa-3') were PCR amplified from N2 genomic DNA and fused to bar-1cDNA::GFP::unc-54UTR fragments.

For *bar-1* constructs a fosmid clone (WRM067af11) was purchased from Source BioScience (Nottingham, United Kingdom) and used as a template to generate genomic PCR fragments. All *bar-1* fragments contained a 4.4kb protein coding region that included exons, introns, and a 3' untranslated region. However, each fragment was driven by a different *bar-1* 5' promoter region. *bar-1* promoter lengths included: 2,666 bp short (S) (5'-agacagattg…tcatggctac-3'), 5,208 bp medium (M) (5'-gaagcctgag…gaattgttga-3'), and 6,908 bp long (L) (5'-tcaatcggca…tcatggctac-3') fragments upstream of the ATG start codon.

All constructs were digested to verify the fidelity of the PCR. Extrachromosomal transgenes were injected at 10ng/µl with 110 ng/µl pBluescriptll and 5 ng/µl of co-injection marker (*myo-3p::mCherry*) using standard methods (Rieckher et al. 2017).

2.3 Embryonic Imaging

Larval L4 worms (10-15 individuals) were transferred to new plates and placed at 25°C overnight. Within 24 hours, the embryo progeny were mounted (10-20 embryos) on agar slides with 4-5 µl of M9 and 25 µm diameter polystyrene beads (Polyscience Inc.). For time-lapse imaging, large beads were chosen to avoid compression of the cover slip on the embryos. As little bacterial lawn as possible was transferred with the embryos onto the slide in order to avoid

oxygen deprivation and pre-mature death. To image embryos at discrete stages (bean stage, 1.5-fold, 2-fold, 3-fold) (Hall et al. 2017), additional bacterial lawn was transferred to hasten hypoxia-induced developmental arrest. This was particularly important after the 1.5-fold stage as embryonic twitching makes imaging impossible. Once slides were prepared, embryos were imaged on a Zeiss AxioImager epifluorescence microscope using a 63x objective. To ensure the embryonic ventral nerve cord remained in focus the plane was manually adjusted before image acquisition. Fluorescent imaging typically involved acquiring 5-10 slices in total with 0.5 μm between slices. A DIC image was also taken at each time point to show the embryonic stage. Embryo circumference was manually traced using Zeiss AxioVision software version 4.8 or in Adobe Illustrator and added to corresponding fluorescent images.

In order to image a relative point between discrete stages of the embryo, we used the embryo's circumference as a measure of development. Embryos elongate from the bean to 3-fold stages. As the size of their outermost layer (eggshell) remains constant, the inner embryo (termed embryo proper) folds upon itself. In order to determine the rate of elongation during embryogenesis a ratio between the circumference of the embryo's eggshell and the embryo proper taken; measured using Zeiss AxioVision software. This ratio [embryo proper/eggshell] increases linearly from the bean to 2-fold stages (Figure A1). Therefore, the ratio is a continuous variable used to describe the 'developmental stage' of the embryo. Even if a mutant grows slower, the comparisons of developmental stage should remain independent of time.

2.4 Larval Imaging

Larval DD and RIG neuron position was determined using a *ynIs37*[*flp-13p::gfp*] and *zyIs27*[*flp-13p*::*gfp*; *unc-129p*::*mCherry*; *myo-2p*::*mCherry*] reporter respectively. Larval stage (L1-L2) worms were immobilized with levamisole (Sigma-Aldrich) to allow for *in vivo* microscopy. Worms were individually imaged using a Zeiss AxioImager epifluorescence microscope on a 20x objective. The position of each DD and RIG neuron was measured using Zeiss Axiovision software. Data was exported from Zeiss Axiovision software into excel to transform the data. Neuron position was converted to percent locations relative to the anterior gut or DD1 and the anus; indicating the 0% AP position and the 100% AP position.

2.5 Data and Statistical Analyses

In-house MATLAB script was used to run statistical analyses and create DD neuron positioning scatter plots. The means and error bars (95% confidence interval) were plotted for each neuron. Two-tailed t-tests were performed for each DD neuron between the mutant and control strains. Significance levels were set as: $p < 0.01$ (*), 0.001 (**). A Fisher exact test was used to compare DD6 axon guidance defects between various genetic backgrounds.

PART 3: RESULTS

3.1 Canonical Wnt-β-catenin components regulate neuron positioning along the AP axis

In *C. elegans* the DA, DB, and DD motor neurons are evenly spaced within the VNC. The stereotypical position of these neurons along the AP axis is the result of a series of regulated cell intercalations events during embryogenesis. One such pathway that aids in cell intercalation during VNC assembly is the non-canonical Wnt/planar cell polarity pathway (Shah et al. 2017). Recent work in our lab suggested that components of the canonical Wnt-β-catenin pathway were involved in positioning neurons in the anterior VNC (Jeffrey Hung and Antonio Colavita, unpublished).

The canonical Wnt-β-catenin pathway consists of five Wnts (*cwn-1, cwn-2, egl-20, mom-2, lin-44),* four Frizzled (*lin-17*, *mom-5*, *mig-1*, *cfz-2*) receptors, three Dishevelleds (*mig-5, dsh-1, dsh-2*), a β-catenins (*bar-1*), and single TCF/LEF factor (*pop-1*)(Jackson et al. 2012). To further investigate how neurons are positioned in the VNC, we examined various Wnt-β-catenin pathway mutants for DD motor neuron spacing defects (Figure 4). *mom-2*/Wnt and *mom-5*/Fz were not assessed due to their known embryonic lethality (Thorpe et al. 1997). Further, a hypomorphic mutant was used as *pop-1* nulls are embryonic lethal (Siegfried et al. 2002).

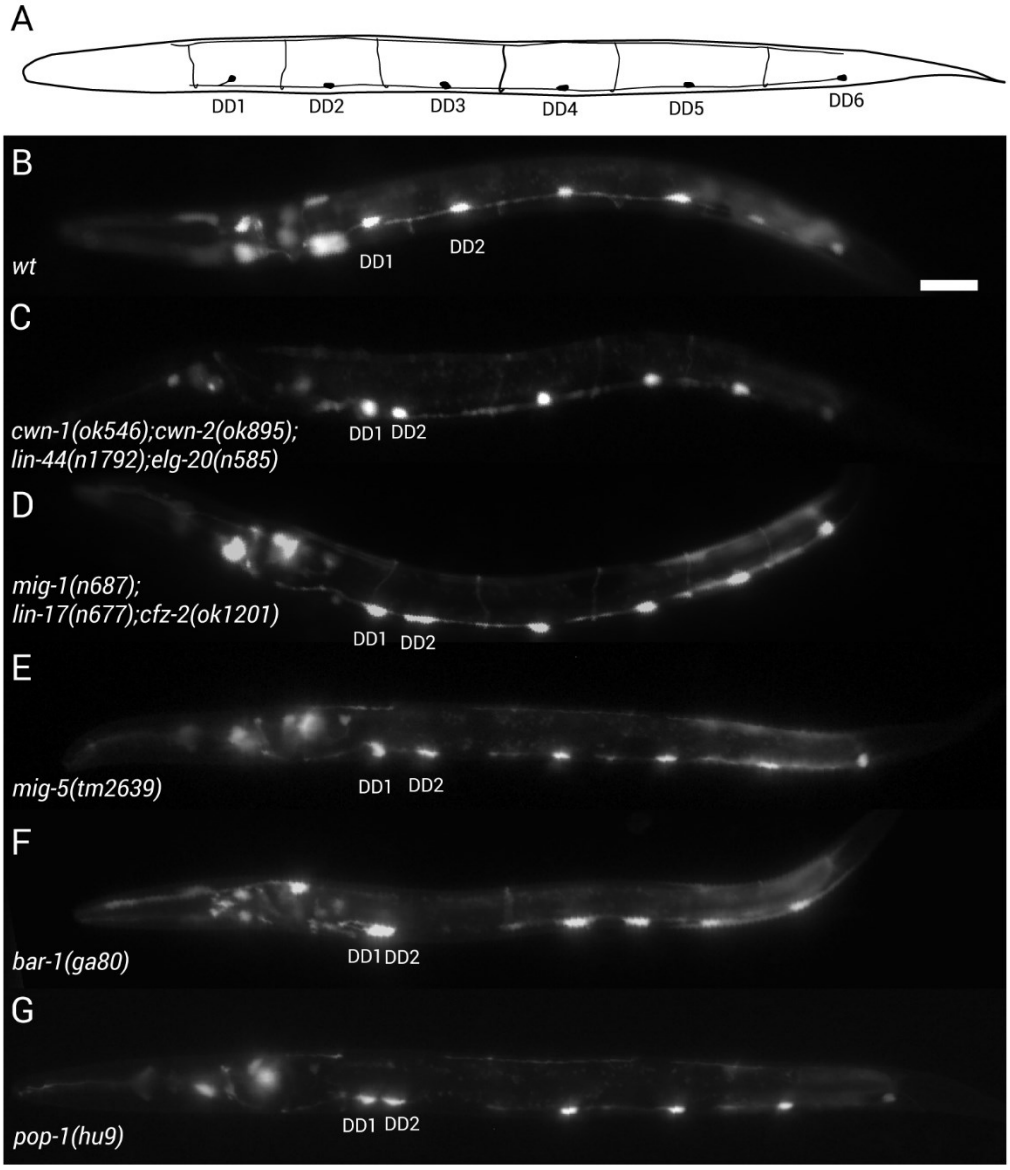

Figure 4. Wnt/β-catenin mutants affect DD neuron position in the ventral nerve cord
(A) A schematic and (B) an image of a representative *wt* worm showing the six DD neurons evenly spaced along the anterior-to-posterior axis in the *C. elegans* ventral nerve cord. (C-G) Anterior shifts in DD2 position are present in strains carrying multiple (Wnts and Frizzleds) or single (MIG-5/Disheveled, BAR-1/β-catenin, POP-1/TCF) mutations in components of the canonical Wnt pathway. DD neurons were visualized using a *ynIs37*[*flp-13p::gfp*] reporter. Scale bar is 20 μm.

The six DD neurons (DD1-6), visualized with a *ynIs37[flp-13p::gfp]* reporter transgene, are evenly spaced in the VNC (Figure 4A).We found that mutations in four individual Wnt ligands (*cwn-1(ok546), cwn-2(ok895), egl-20(n585), lin-44(n1792)*), with the exception of an anterior shift in DD4 position in *cwn-1(ok546)* mutants, most showed normal DD spacing. However, disruption of multiple Wnt ligands, as in the quadruple mutant *cwn-1(ok546); cwn-2(ok895); lin-44(n1792); egl-20(n585)* showed significant DD spacing defects including an anterior shift in the average position of DD2 (Figure 4C and Figure 5). Similarly, at the receptor level, individual Frizzled mutants did not exhibit DD position defects whereas the triple mutant *lin-17(n677)*; *mig-1(n678)*; *cfz-2(ok1201)* showed mild DD position defects including an anterior shift in the average position of DD2 (Figure 4D and Figure 5). This suggest that Wnt ligands and Frizzled receptors act redundantly in specifying the position of DD neurons along the AP axis. In contrast, disrupting downstream components exhibited severe DD position defects. The null mutants *mig-5(tm2639)* and *bar-1(ga80)*, and a *pop-1(hu9)* hypomorphic mutant all exhibited anterior DD2 neuron spacing defects (Figure 4 and Figure 5). Therefore, we can conclude that canonical Wnt-β-catenin components are important for specifying DD2 position along the AP axis.

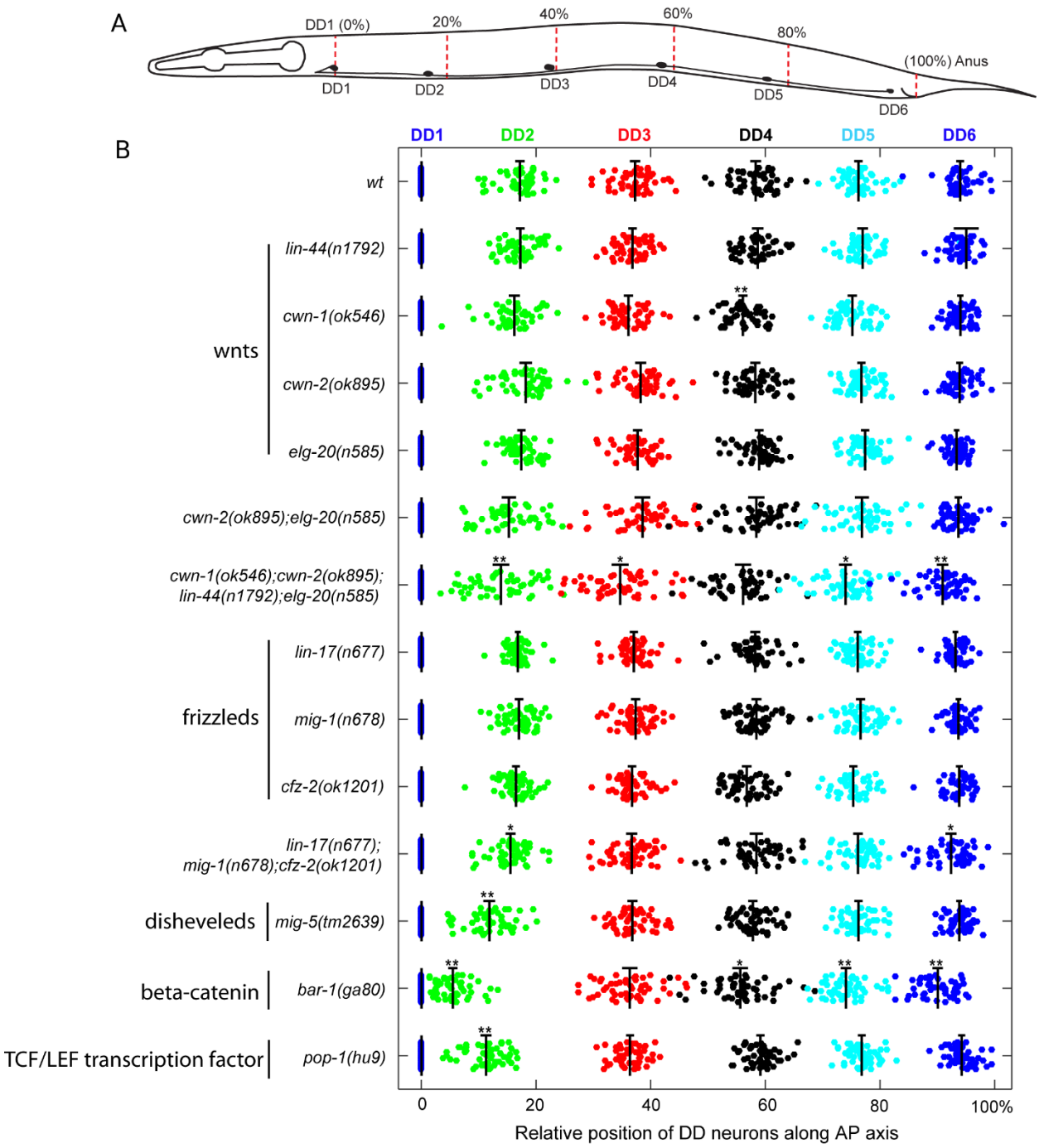

Figure 5. Wnt/β-catenin components affect DD2 neuron position
(A) A schematic showing the six DD neurons along the anterior-to-posterior axis. Neurons are plotted along the anterior-to-posterior axis where DD1 is the 0% AP position and the anus is the 100% AP position. Each DD neuron has a mean (vertical black line) and 95% confidence interval (horizontal black line). (B) DD neuron spacing in wt and various Wnt pathway mutants. 50 animals were scored per strain. Significance, $p < 0.01$ (*), 0.001 (**) using two-tailed t tests.

3.2 pry-1/axin mutants display anterior shifts in the position of DD1

Our genetic analyses suggest that reduced Wnt signaling, for example loss of *bar-1*/β-catenin, results in an anterior shift of DD2 towards DD1. We next asked how increased Wnt signaling would affect DD positioning. Under normal conditions, the APC/Axin destruction complex targets free β-catenin for proteasome-mediated degradation (Fagotto 2013). Therefore, we examined DD neuron spacing in a *pry-1*/Axin mutant which is predicted to increase BAR-1 levels due to loss of the destruction complex (Korswagen et al. 2002). Interestingly, in *pry-1(mu38)* mutants, instead of DD2 position defects, DD1 was shifted posteriorly towards DD2 (Figure 6A,B). Both *bar-1(ga80); pry-1(mu38)* and *pop-1(hu9)*; *pry-1(mu38)* double mutants were able to suppress the *pry-1* DD1 phenotype. This result is consistent with PRY-1 acting upstream of BAR-1 and POP-1/TCF (Figure 6D). Together, these findings suggest that BAR-1 levels are tightly regulated in order to achieve proper spacing of DD1 and DD2 neurons in the VNC.

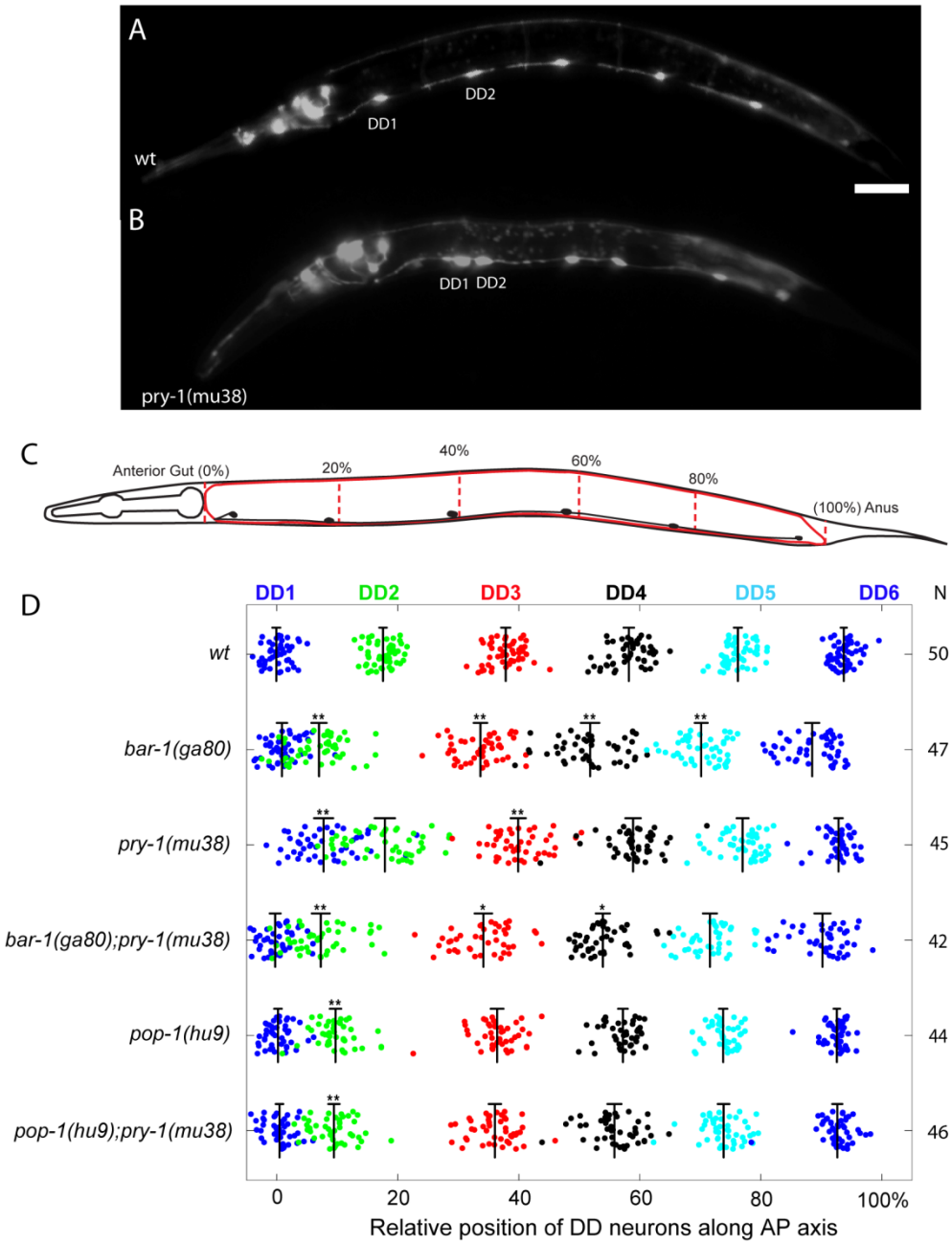

Figure 6. *pry-1/Axin* mutants display a posterior displacement of DD1 that is suppressed in *bar-1*/β-catenin and *pop-1*/TCF double mutants

(A) Evenly spaced DD neurons in the *wt* worm. (B) DD1 is displaced posteriorly in *pry-1(mu38)* mutants. DD neurons were visualized using the *ynIs37[flp-13::gfp]* reporter. Scale bars are 20 µm. (C) A schematic showing DD neurons. DD neurons are plotted relative to the anterior gut (0% AP position) and anus (100% AP position). (D) Loss of β-catenin and its target POP-1/TCF suppresses the β-catenin-overexpression phenotype in the double mutants *bar-1(ga80); pry-1(mu38)* and *pop-1(hu9); pry-1(mu38)*. The number of animals scored (N) is specified right of the axis. Significance: $p < 0.01$ (*), 0.001 (**) using the two-tailed t test.

3.3 RIG neurons display position defects in bar-1 and pry-1 mutants

Both Wnt and their Frizzled receptors are known to specify neuron position in the mid-body region (Pan et al. 2006; Zinovyeva et al. 2008). Here, we investigated whether the Wnt-β-catenin pathway affects additional neuron positions in the anterior body region. We chose to look at the RIG neurons as they are sister cells of DD1 and DD2. The AB.prppappa (RIGR, DD2) and AB.plppappa (RIGL, DD1) lineages adopt an AP order in the VNC with RIGR, DD1, RIGL in a cluster and DD2 further posterior along the AP axis (Figure 7A). Therefore, we wanted to determine whether RIG neuron position was also affected in *bar-1* mutants. To test this hypothesis we used a *zyIs32*[*flp-13::gfp; flp-18::rfp*] reporter background to label DD neurons with GFP and the RIG neurons with RFP. We showed that *bar-1(ga80)* mutants retained their alternating RIG/DD order (Figure 7E), but that RIGL is displaced towards DD2. Additionally, both RIGs are displaced posterior in *pry-1(mu38)* mutants (Figure 7F). One possibility is that RIG neuron position defects are caused by cell fate changes, as the Wnt-β-catenin pathway is known to drive binary cell fate decisions required for proper AP axis formation (Bertrand 2016). However, this is unlikely as the number of RIG (*flp-18::gfp*) or DD (*flp-13::rfp*) neurons labelled by each reporter did not change in *bar-1* mutants. We can therefore conclude that RIG and DD neurons do not regulate their position along the AP axis through simple Wnt-β-catenin-directed cell fate decisions. Rather, these results suggest that the Wnt-β-catenin pathway helps regulate multiple neuron positions in the anterior body region.

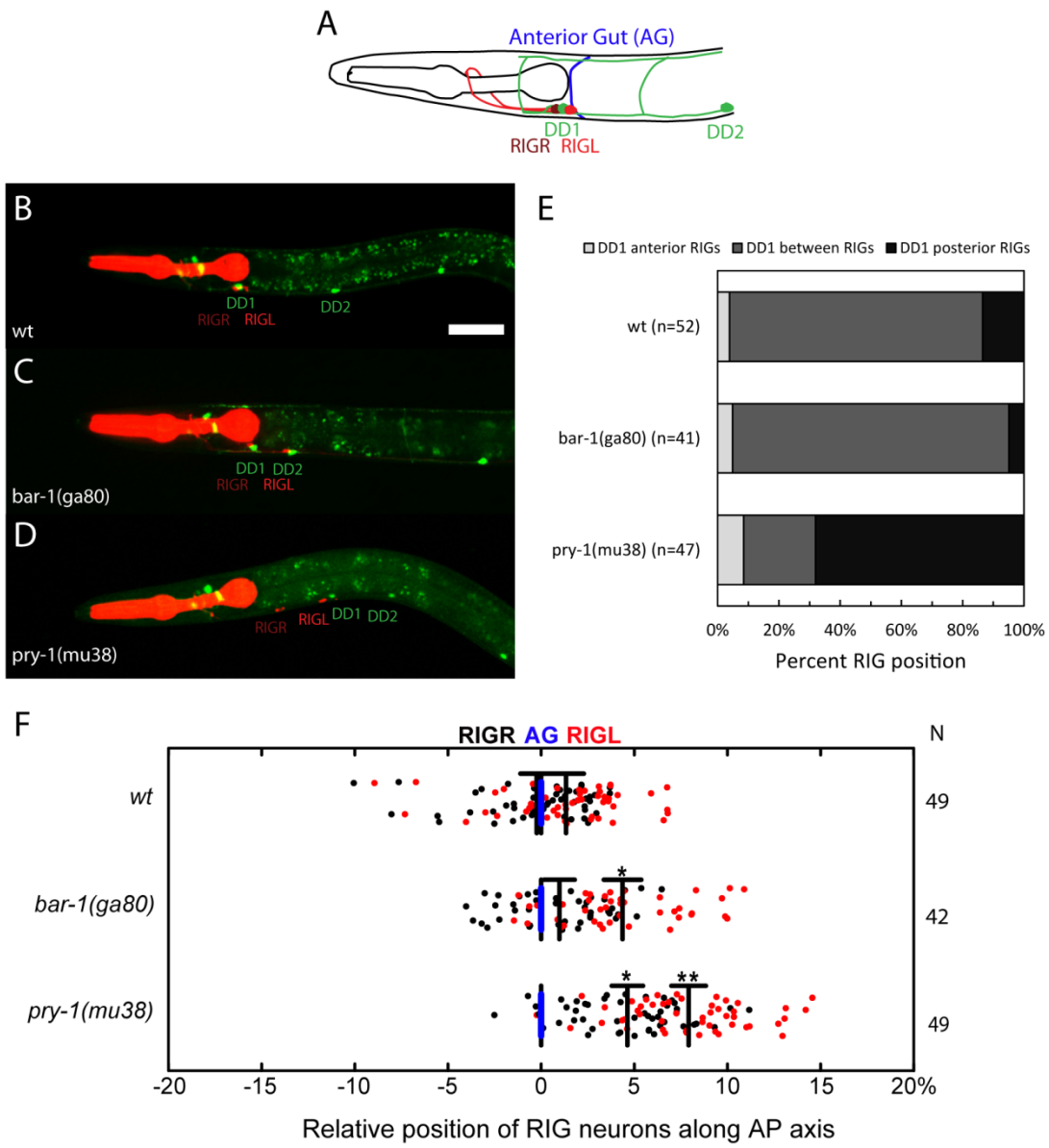

Figure 7. β-catenin regulation does not induce cell-fate switches in DD neurons
(A) The sister cells RIGR and DD2 and RIGL and DD1 adopt the anterior-to-posterior order: with RIGR, DD1, RIGL in a cluster and DD2 further posterior along the anterior-to-posterior axis. The schematic shows DD and RIG neurons relative to the anterior gut (AG). (B-D) Representative *wt* and mutant worms in which DD (green) and RIG (red) neurons are labeled with a *zyIs32[flp-13::gfp; flp-18::rfp]* reporter. (E) *bar-1(ga80)* mutants retain their anterior-to-posterior RIG and DD order despite an anterior position of DD2, whereas DD1 is posterior to the RIGs in *pry-1(mu38)* mutants. Scale bars are 20 µm. (F) In *bar-1(ga80)* mutants, RIGR is posterior towards DD2, whereas both RIGR and RIGL are posteriorly in *pry-1(mu38)* mutants. RIG neuron quantification was the same as in Figure 4D. The number of animals scored (N) is specified right of the axis. Significance: $p < 0.01$ (*), 0.001 (**) using the two-tailed t test.

3.4 bar-1/β-catenin is expressed in epidermal cells and neurons during body axis extension

Next, we wanted to determine the expression pattern of *bar-1*/β-catenin to gain insight into where it may be acting to regulate DD neuron position. We therefore decided to generate a transgenic line expressing a BAR-1 translational fused to GFP (*BAR-1::GFP*) driven by a *bar-1* promoter. To ensure that the *bar-1* promoter contained the necessary regulatory elements required for proper DD positioning, we first carried out a rescue experiment using various *bar-1* genomic PCR fragments. Each of the three *bar-1* genomic fragments had the same coding region (4.8kb) but varying promoter lengths: a short (S) 2.7 kb, medium (M) 5.2 kb, and a long (L) 6.9 kb promoter (Figure 8A). We found that only the medium and long *bar-1* genomic lines were able to rescue DD spacing defects (Figure 8B). We therefore made a translational *bar-1p::bar-1::gfp* (zyEx80) reporter. We show that our zyEx80 (5.1kb *bar-1* promoter + cDNA) reporter and *bar-1* genomic PCR fragment (M) (5.2kb *bar-1* promoter + genomic open reading frame) line both rescue DD spacing defects to a similar degree (Figure 8B and Figure 9A,B). Further, zyEx80 was able to rescue two independent *bar-1* null alleles, ga80(Q97stop) and mu350(Q143stop) (Figure 9B,C). In addition, zyEx80 rescued DD neuron axon guidance defects (Figure 1S) that are also a prominent feature of *bar-1* null mutants (Maro et al. 2009). These results indicate that the *BAR-1::GFP* fusion is functional and is driven by a *bar-1* promoter that contains the requisite regulatory elements important for DD neuron positioning and axon guidance.

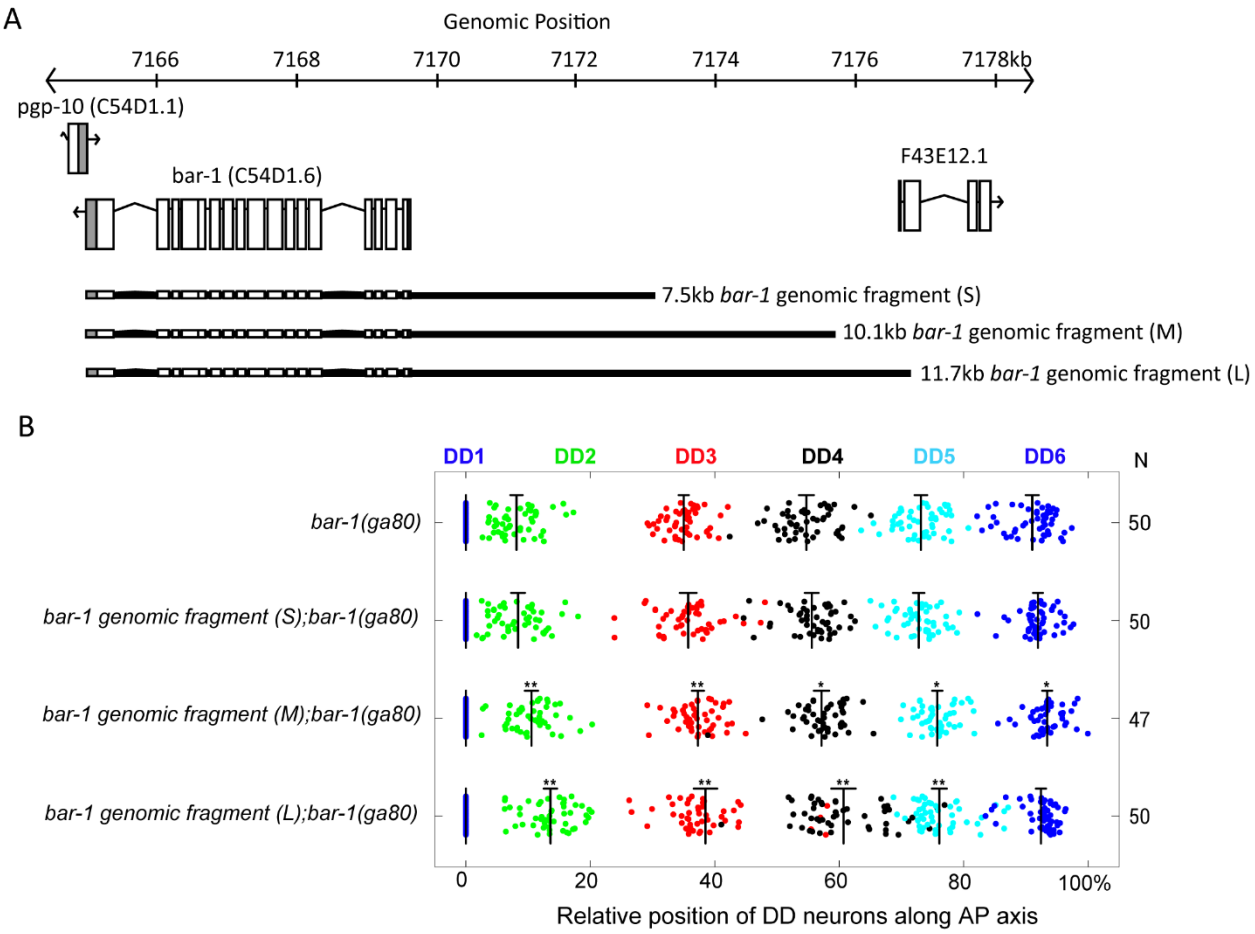

Figure 8. Rescue of *bar-1* DD position defects using genomic fragments
(A) A schematic of the *bar-1* genomic region between pgp-10(C54D1.1) and F43E12.1. Various lengths of *bar-1* genomic DNA were tested for rescue of *bar-1(ga80)* DD position defects. Each PCR fragment contained the full *bar-1* coding region but varying promoter lengths: a short (S) 2.7 kb, a medium (M) 5.2 kb, and a long (L) 6.9 kb promoter. (B) Only the medium and long genomic fragments rescue DD spacing defects. DD neuron quantification was the same as in Figure 4B. Each DD neuron has a mean (vertical black line) and 95% confidence interval (horizontal black line). The number of animals scored (N) is specified right of the axis. Significance: $p < 0.01$ (*), 0.001 (**) using two-tailed t tests.

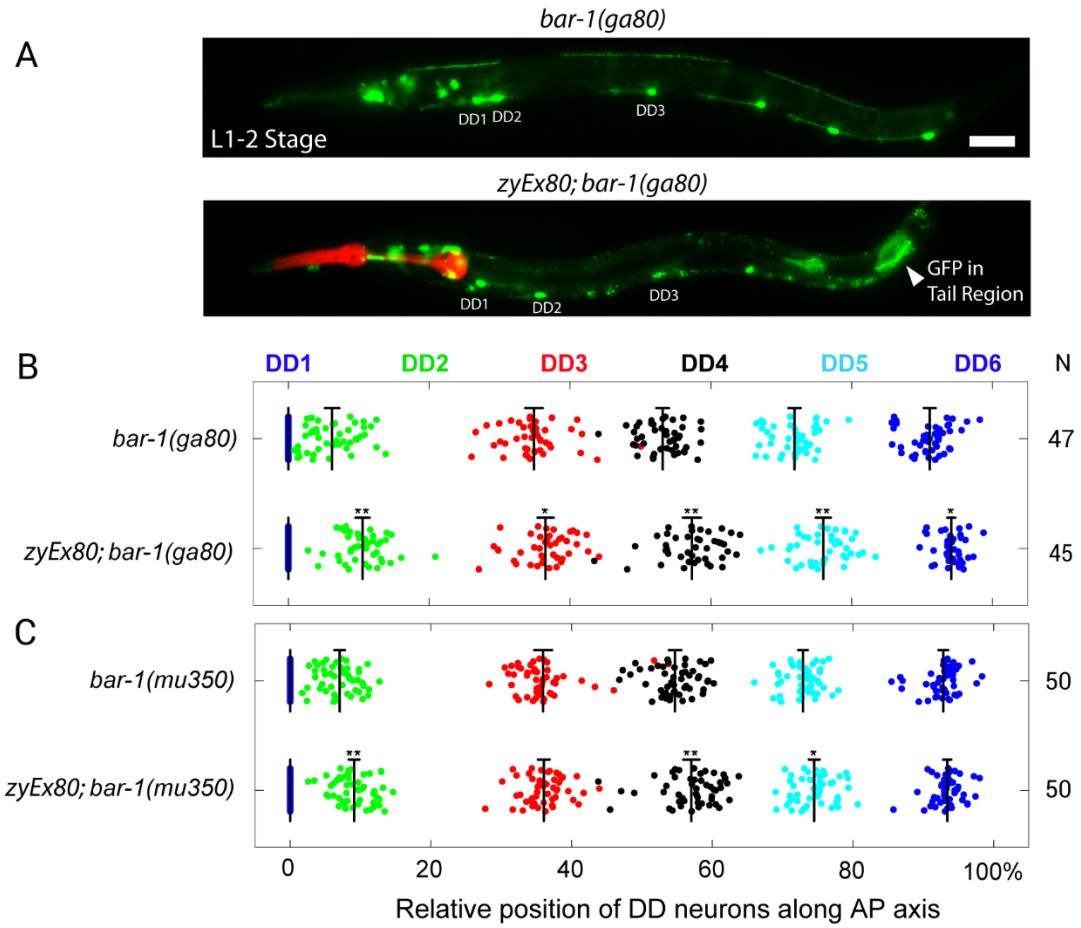

Figure 9. BAR-1::GFP rescues DD spacing defects in *bar-1* mutants
(A) Transgenic expression of a BAR-1::GFP fusion (*zyEx80*) is able to rescue DD neuron spacing defects in *bar-1(ga80)* mutants. White arrow indicates BAR-1 expression in the tail. DD neurons were visualized using the *ynIs37[flp-13::gfp]* reporter. Scale bar is 5 µm. (B,C) The BAR-1::GFP fusion is able to rescue both *bar-1(ga80)* and *bar-1(mu350)* null mutants. DD neuron quantification was the same as in Figure 5B. Each DD neuron has a mean (vertical black line) and 95% confidence interval (horizontal black line). The number of animals scored (N) is specified right of the axis. Significance: $p < 0.01$ (*), 0.001 (**) using two-tailed t tests.

We next examined the expression pattern of BAR-1::GFP (zyEx80) (Figure 10). As DD neuron position defects are present at hatching (Larval stage 1 (L1)) in *bar-1* mutants, we assessed expression in embryos and at the L1 stage. During morphogenesis the embryo undergoes several distinct phases before it can emerge from its eggshell. At approximately 360 minutes post-fertilization the embryo starts to change from a round shape into a more elongated worm-like shape. These stages are broken down into the bean stage, comma stage, 1.5-fold stage, 2-fold stage, and 3-fold stage. From as early as the bean stage (data not shown), *bar-1* appeared to be expressed in epidermal seam cells and neurons in the head region. This expression persisted into to the comma stage (Figure 10A.1), and through development. However, in the VNC *bar-1* expression was not observed until the 1.5-fold stage, when we found a single BAR-1::GFP positive cell ventral to DD1 and DD2 (Figure 10A.2). Given the latency involved with GFP chromophore maturation (Cormack BP, Valdivia RH 1996), BAR-1::GFP is likely active before the 1.5-fold stage. We also found BAR-1::GFP positive cells at the 2-fold (Figure 10A.3) and 3-fold stages (Figure 10A.4). While we know the post-embryonic order of VNC neurons - RIGR, DD1, RIGL, DA1, DB3, DA2, DD2, DA3, DB4, DA4, DD3 – further work would be needed to verify the specific cell identify of the BAR-1::GFP positive cells. BAR-1::GFP is also expressed in DA2, DA4, DA5, DD5, and four additional GFP positive cells (likely DBs) by the 3-fold stage (Figure 10A.4). At the post-embryonic L1 stage *bar-1* is expressed many VNC neurons (Figure 10B,C).

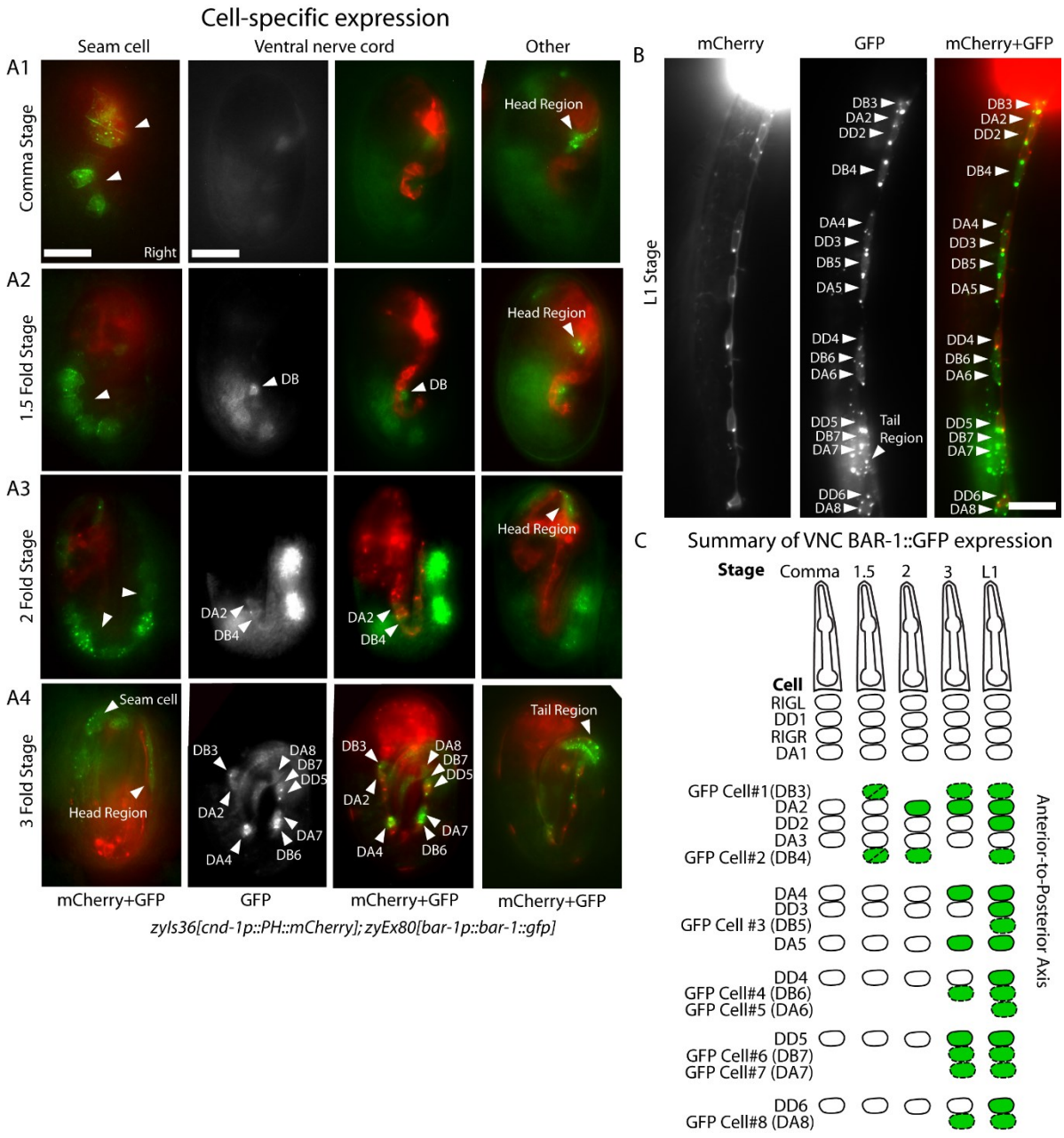

Figure 10. BAR-1::GFP is expressed in DD, DA, and DB neuroblasts during embryogenesis (A-D) Images of various embryonic stages showing a subset of neuroblasts labeled with a *cnd-1p::PH::mCherry* reporter and BAR-1::GFP (*zyEx80*) expression. (B) At the embryonic comma stage BAR-1 expression is limited to epithelial seam cells, cells in the head region, but no visible expression in or near the ventral nerve cord. At the 1.5-fold (C) and 2-fold (D) stages BAR-1::GFP is expressed in a single neuroblast (tentatively identified as a DB neuron). (E) By the 3-fold stage, BAR-1::GFP is expressed in several neurons along the VNC. (F) BAR-1::GFP continues to be expressed in neurons along the VNC in L1 animals. Scale bars are 10 µm.(G) Schematics showing a summary of BAR-1::GFP expression. *cnd-1p::PH::mCherry* (solid black), BAR-1::GFP positive cells (green), non-*cnd-1p::PH::mCherry* cells with BAR-1::GFP (dashed black, green).

3.5 bar-1/β-catenin acts in neurons to regulate DD neuron position in the VNC

As *bar-1* was found to be expressed in neurons and epidermal cells we sought to determine where *bar-1* was required to regulate the position of DD neurons in the VNC. We therefore decided to drive *bar-1* expression from cell-specific promoters and assess their ability to rescue DD neuron position defects in *bar-1* mutants. We used an *unc-33* promoter (Tsuboi et al. 2005) and a *dpy-7* promoter (Myers et al. 2007) to drive pan-neuronal and pan-epidermal *bar-1* expression respectively. We found that BAR-1 expressed in neurons but not epidermal cells were able to rescue DD spacing defects (Figure 11). These findings suggest that *bar-1* is required in neurons to regulate DD neuron position.

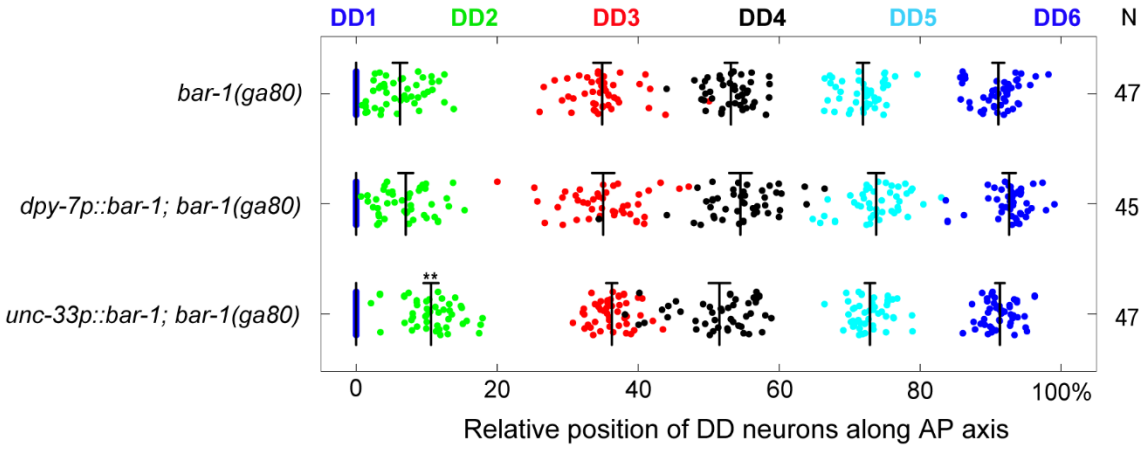

Figure 11. BAR-1 acts in neurons to regulate DD neuron spacing
Expression of BAR-1 using *unc-33* (pan-neuronal) and *dpy-7* (epidermal) cell-specific promoters. *bar-1* expression in neurons but not epidermal cells was able rescue DD spacing defects in *bar-1(ga80)* mutants. DD neuron quantification was the same as in Figure 5B. Each DD neuron has a mean (vertical black line) and 95% confidence interval (horizontal black line). (N) is indicated on the right. Significance: $p < 0.01$ (*), 0.001 (**) using two-tailed t tests.

3.6 β-catenin affect single-cell intercalation during embryonic convergent extension of the VNC

In *C. elegans*, neuron position in the VNC requires a regulated series of cell intercalation events. When neuroblasts first meet at the ventral midline they undergo a set of multicellular processes (Figure 12B). Further cell constrictions along the midline force neuroblasts to sort along the AP-axis. At the 1.5-fold stage neuroblasts start undergoing single-celled intercalations. Final intercalation events between the 2 and 3-fold stages result in neuroblasts forming a single file along the AP-axis. Disruption of PCP signaling results in multicellular intercalation defects during VNC formation. These defects affect neuron spacing along the AP-axis (Shah et al. 2017). We therefore sought to determine whether *bar-1* regulates cell intercalation events during VNC development. First, we conducted time-lapse microscopy in a *zyIs40*[*unc-30p::gfp cnd-1p::PH::mCherry*] reporter background to trace the lineage of DD1 and DD2 and their sister neurons (RIGL and RIGR) (Figure A2). Then, we found that the single-celled intercalation events during the 1.5- to 2-fold stages contribute to the proper spacing of DD1 and DD2 neurons in the VNC (Figure 12C,D). While DD1 and DD1 are in physically contact with each other at the 1.5-fold stage, they become separated by the 2-fold stage (8/8 *wt* embryos with 2 cells between DD1 and DD2). This spacing increases as the embryo elongates at the 3-fold stage (6/6 *wt* embryos) (Figure 12E). In *bar-1(ga80)* and *pry-1(mu38)* mutants neuroblasts are correctly positioned at the 1.5-fold stage. However, DD1 and DD2 are not- or incorrectly separated by the 2-fold stage (5/9 *bar-1* embryos; 6/10 *pry-1* embryos). Further, the spacing of DD1 and DD2 does not improve with elongation of the body axis at the 3-fold stage (4/8 *bar-1* embryos; 4/10 *pry-1* embryos). Together, this data helps specify a discrete window when the mispositionioning of neurons in *bar-1* mutants arise.

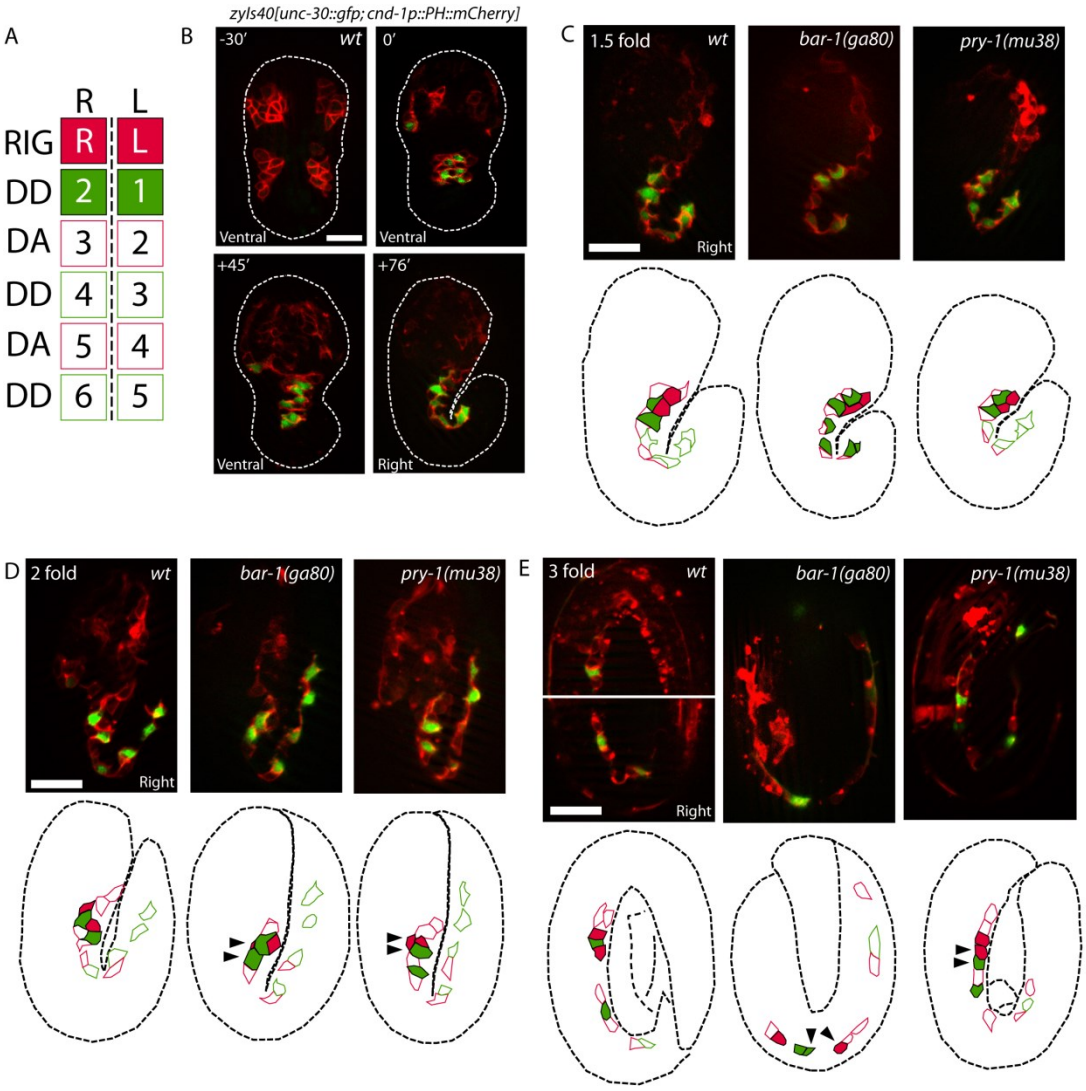

Figure 12. *bar-1/*β-catenin regulates single-celled intercalation during convergent extension of the ventral nerve cord

(A) The color key is organized based on the relative left-right configuration of the RIG, DD, and DA neurons. (B) *C. elegans* embryos with a *zyIs40*[*unc-30p::gfp cnd-1p::PH::mCherry]* reporter where cytoplasmic GFP labels DD neurons and membrane-bound mCherry that labels a subset of neuroblasts (including DA and DD neurons). Four representative images show that convergent extension of the VNC involves the migration of neurons along the medial-lateral axis, single-celled intercalation, and extension along the anterior-to-posterior axis. White dashed contour outline the embryos. (C) Traced outline of a representative *wt*, *bar-1(ga80)*, and *pry-1(mu38)* embryos. Identification of RIG neurons in each representative embryo was estimated based on independent time-lapse following DD and RIG sister cells through development (pre-bean to 1.5-fold stages). At the 1.5-fold stage DD1, DD2, RIGL and DA2 meet at a central vertex. (D) At the 2-fold stage, defects in single-celled intercalation results in DD2 moving anterior towards DD1 in *bar-1(ga80)* mutants, and DD1 moving posterior towards DD2 in *pry-1(mu38)* mutants. Black arrows indicate defects. (E) These defects persist during extension along the anterior-to-posterior axis. Scale bars is 10 μm.

3.7 β-catenin affect cell neighbor-exchanges during single-celled intercalation of the VNC

Based on our finding that Wnt-β-catenin mutant defects arise between the 1.5-to 2-fold stages, we used our time lapse imaging approach to more closely examine the specific cell-intercalation events involving DD1 and DD2. We found that DD1, RIGL, DD2, and DA2 are in close contact with each other during this time frame. The spatial separating DD1 and DD2 along the AP axis involves a process by which RIGL and DA2 intercalate between the DDs. This process is known as a T1-transition cell neighbor exchange. First, constriction of the DD1 and DD2 cell junction along the dorsal-ventral (DV) axis forms a central vertex with DD1, RIGL, DD2, and DA2 (Figure 13A). The resolution of the central vertex occurs from the anterior-posterior expansion the RIGL and DA2 cell junction (Figure 13B). The result of the T1 transition is the spatial separation of DD1 and DD2 along the AP axis. However, in Wnt-β-catenin mutants the central vertex resolves back into its pre-vertex configuration, resulting in the reformation of the DD1 and DD2 cell junction along the DV axis (Figure 13C). In *bar-1(ga80)* mutants there is no bias towards a DV or AP resolution following vertex formation. In contrast, nearly all *pry-1(mu38)* mutants revert to their pre-vertex configuration, through DV resolution. We also verified that β-catenin regulation of T1 transitions are independent of developmental timing (Figure A3). These findings suggest that DD and RIG neuron position defects are a function of canonical Wnt-β-catenin activity biasing the resolution of T1 transitions during cell-intercalation during VNC assembly.

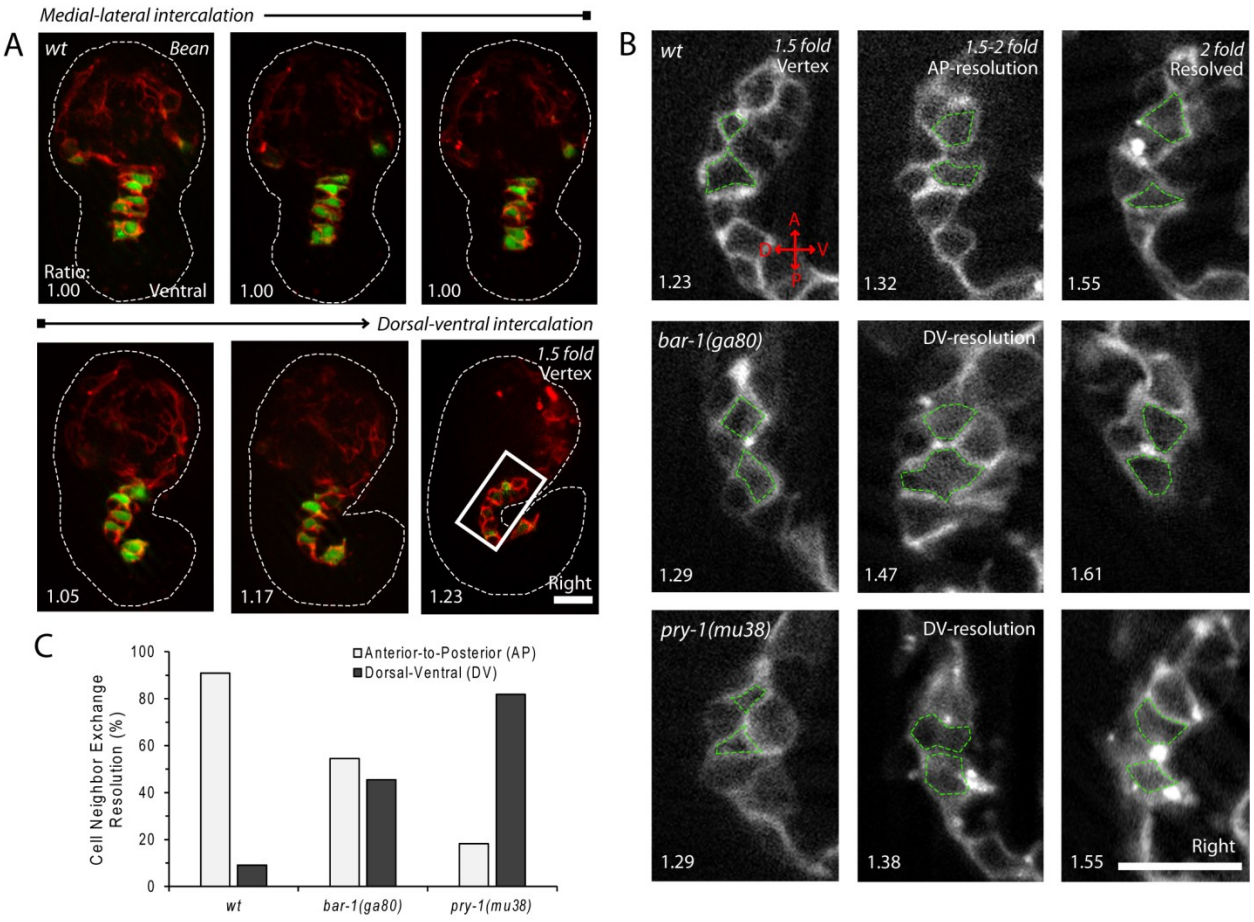

Figure 13. *bar-1*/β-catenin regulates the resolution of T1-transition cell neighbor exchanges during single-celled intercalation

C. elegans embryos with a *zyIs40*[*unc-30p::gfp cnd-1p::PH::mCherry]* reporter. White dashed contour outline the embryos. (A) Single-celled intercalation of the VNC involves cell-neighbor exchanges (also called T1 transitions). Single slices of embryos show an example of a T1 transitions involving four cells in the VNC. The dorsal-ventral (DV) constriction of the DD1 and DD2 cell junction, during the bean stage, leads to a central vertex between DD1, DD2, RIGL and DA2 neurons. Note the embryo rotates from a ventral to right side view during this time frame. Scale bar is 5 μm. (B) Resolution of the central vertex, through the creation of an anterior-to-posterior (AP) vertex between RIGL and DA2, results in the spatial separation of DD1 and DD2 in *wt* embryos. Scale bars is 10 μm. (C) Overexpression of β-catenin (in *pry-1* mutants) biases the resolution towards a DV vertex formation, whereas there is no bias between DV or AP vertex formation when β-catenin is lost (in *bar-1* mutants). 11 animals were scored per genotype. Significance: $p < 0.05$ using a two-tailed t test.

PART 4: DISCUSSION

4.1 Redundancy among Wnt/Fz components in DD neuron position

Wnt signaling is an evolutionarily conserved cascade that aids in the positioning of cells along the body axis (Schambony A 2003). It has been recently shown in *C. elegans* that Wnt/PCP signaling is involved in the positioning of neurons along the AP axis in the VNC (Shah et al. 2017). Here, we have investigated the role of Wnt/β-catenin signaling in positioning DD motor neurons (Figure 14). We found that proper DD neuron positioning involves redundancy among Wnt genes. Disruption of four Wnt ligands or three Frizzleds were necessary to cause anterior DD2 position defects. In *C. elegans*, Wnt genes have been shown to exhibit functional redundancies during cell fate establishment (Gleason et al. 2006), growth cone migration (Pan et al. 2006), and cell migration (Zinovyeva and Forrester 2005, Zinovyeva et al. 2008). Here, we showed that downstream Wnt components also exhibit spacing defects, which supports our finding that the canonical Wnt/β-catenin pathway is involved in regulating DD neuron spacing.

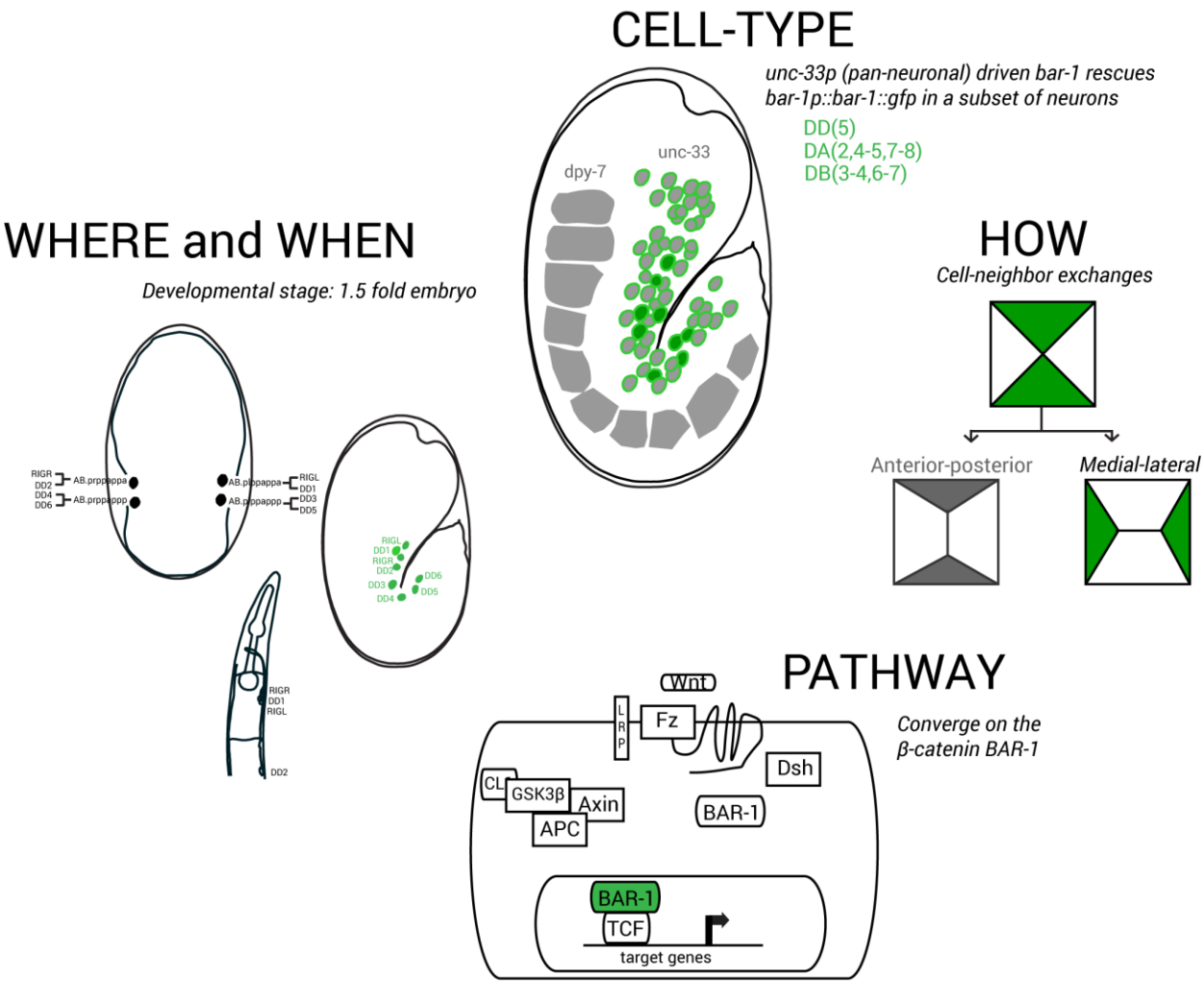

Figure 14. A summary of the role of the Wnt/β-catenin pathway in positioning DD neuron along the ventral nerve cord

Loss of canonical Wnt/β-catenin components (Wnts, Frizzleds, Dishevelled, β-catenin, and TCF) result in DD spacing defects. *bar-1*/β-catenin mutants display DD neuron spacing defects after the embryonic 1.5-fold stage. BAR-1 is required in neurons for proper DD neuron spacing. *bar-1* mutants do not exhibit proper T1-transition cell neighbour exchanges between DD1, DD2, RIGL and DA2 neuroblasts. In *bar-1* mutants the vertex resolves along the dorsal-ventral axis instead of the anterior-to-posterior axis.

4.2 bar-1/β-catenin acts in neurons to regulate DD neuron spacing

Here, we've shown that *bar-1*/β-catenin is acting in a Wnt-mediated process to regulate DD neuron position in the VNC. *bar-1* was expressed in epidermal seam cells, DA and DB neurons in the ventral nerve cord, as well as several cells in the head and tail region in the embryo. This result is consistent with previous findings that *bar-1* is expressed in the vulval epidermal cells and in the ventral nerve cord (Natarajan et al. 2004). We've also shown that, in these cells, BAR-1 is not concentrated in the nucleus despite its role as a transcription cofactor, but instead localized to both the cytoplasm and nucleus in equal measure. This result is consistent with previous studies showing that β-catenin is free to enter and exit the nucleus independent of classic nuclear transport receptors (Wang et al. 2014; Wiechens et al. 2001). Using cell-specific lines, we further showed that pan-neuronally driven *bar-1* rescued *bar-1* mutant DD spacing defects. This indicates that BAR-1 acts in neurons to regulate DD spacing. However, due to the lack of neuron-class specific promoters, we do not know if BAR-1 is required autonomously in the DD neurons or non-autonomously in adjacent neurons (such as DA or DB) to ensure proper DD neuron spacing.

4.3 β-catenin regulates neuroblast cell intercalations during VNC assembly

Cellular junctional integrity and tissue architecture is maintained by the cell adhesion and binding functions of adherens junctions (Lecuit et al. 2015). E-cadherin, a transmembrane protein, binds a complex of α and β-catenin via its intracellular domain. This complex links

extracellular adhesive contacts with the intracellular actin cytoskeleton. Thus, the cadherin-catenin complex (CCC) is used to bind neighboring cells (Mege et al. 2017). In *C. elegans,* as well as in other animals, β-catenin proteins play two distinct roles, one in adhesion and the other in Wnt signaling (McCrea et al. 2010). Here we have shown that the Wnt-β-catenin-pathways is involved in DD neuron spacing.

Our principal finding is that BAR-1/β-catenin levels affects junctional rearrangements during single-cell intercalation in the VNC. We showed that a specific cell-neighbor exchange (known as a T1 transition) involving the DD1, DA2, RIGL and DD2 neuroblasts was defective in *bar-1* mutants. Normally, this T1 transition resolves with an expansion of the DA2 and RIGL vertex along the AP axis. This resolution results in the separation of DD1 and DD2. Loss of BAR-1 resulted in T1 transitions that fail to properly resolve along the AP axis, with about half of vertices reverting to their pre-vertex morphology; resolving along the DV axis. Whereas in *pry-1/Axin* mutant, which is predicted to increase the levels of β-catenin, nearly all T1 transitions reverted to their pre-vertex morphology. This suggests the Wnt/β-catenin pathway aids in the polarization of DD neuron T1 transitions in the embryo.

In VNC assembly, the non-canonical PCP pathway has also been implicated in polarized cell movements. Prior to neuroblasts meeting at the ventral midline, DA and DD neuroblasts undergo a stereotyped neighbor exchange such that the posterior edge contraction of DD4 results in DA5 intercalating between DD4 and DD6. However, in PCP pathway mutants the anterior edge of DD4 contracts, resulting in improper cell-cell contacts. PCP mutants also affect the common intermediary structures known as rosettes (Shah et al. 2017). Multiple junctions are required to collapse simultaneously for cells to interface at the focal point of the rosette. In contrast to canonical Wnt/β-catenin defects, which exhibit a single, discrete single-cell

intercalation defect, PCP mutants defects are more wide-spread and severe by the same developmental stage (Shah et al. 2017). Thus, it is not surprising that PCP pathway mutants exhibit not only anterior DD2 spacing defects, but also DD3, DD4, DD5, and DD6 defects (Shah et al. 2017).

Whether the PCP pathway regulates Wnt/β-catenin signaling in our model remains to be determined. However, the Wnt/β-catenin and PCP pathways have been shown exhibit cross-talk at the receptor level. In *Drosophila*, the Wnt co-receptor Lrp6 can bind to the scaffolding protein Axin, a component of the destruction complex, and inhibit the degradation of β-catenin (Tamai et al. 2004). However, in *Xenopus,* Lrp6 was shown to regulate, via its inhibition of PCP signaling, convergent extension mediated neurulation. Inhibition of PCP signaling through Lrp6 was also shown to potentiate Wnt/β-catenin dependent body axis formation, suggesting Lrp6 acts as a switch between the two pathways (Tahinci et al. 2007). Similarly, the adhesion molecule CD146 was shown to act as a Wnt receptor during convergent extension-mediated gastrulation in zebrafish. Not only does CD146 contain a binding region for dishevelled, a core PCP component required for activating the c-Jun amino-terminal kinase (JNK), but it also negatively regulates the canonical Wnt/β-catenin at the β-catenin level (Ye et al. 2013). The ability of PCP components to negatively regulate canonical Wnt/β-catenin is not uncommon (Westfall et al. 2003; Weidinger et al. 2003). Given these findings, it would be interesting if the PCP pathway and Wnt/β-catenin signaling cooperated to ensure proper positioning of all motor neurons in the VNC.

Defects in the polarization of junctional rearrangements are also seen in *Drosophila*. During embryogenesis the germ band increases two-fold along the AP axis while shrinking along the dorsal surface. At the cellular level during germ band extension (GBE), a convergent

extension-mediated process, the number of cells increase along the AP axis while decreasing along the DV axis (Hartenstein et al. 1985). Intercalating cells in the germ band undergo T1 transitions to change cell contacts. Cell junctions oriented along the dorsal-ventral axis shrink to form vertices composed of four cells. Subsequent resolution of these four-cells result from an extension of vertices along the AP axis (Bertet et al. 2004; Zallen et al. 2004; Tamada et al. 2012). Disruption of the gap junction gene Krüppel results in a failure of proper GBE. In Krüppel mutants, T1 transitions lose their unidirectional resolutions, resulting in the formation of randomly resolved cell-cell junctions. In certain instances, T1 transitions also revert back towards their original pre-vertex morphology (Bertet et al. 2004). These defects resemble those that we observe in *bar-1* mutants, where T1 transitions lose their unidirectional resolutions.

The asymmetrical distribution of Arm/β-catenin also affects cellular junctional rearrangements in the *Drosophila* GBE. The non-receptor tyrosine kinase Abl, which is linked to neural tube defects in mice (Koleske et al. 1998), promotes the phosphorylation of Arm/β-catenin (Tamada et al. 2012). In *abl* mutants the polarization of Arm/β-catenin along DV, but not AP, junctions is disrupted. Disruption of Abl also affects whether intercalating cells form rosette intermediaries (Tamada et al. 2012). During GBE, rosette frequency and directionality are necessary for proper tissue elongation. While the collapse of DV cell junctions in rosette formation normally requires actomyosin (Blankenship et al. 2006), defects in in *abl* mutants are independent of actomyosin (Tamada et al. 2012). This suggests actomyosin alone is not the driving force behind junctional remodeling. Previous studies have shown that the scaffolding protein Bazooka/PAR-3 and E-cadherin are enriched along DV cell interfaces, whereas myosin-II is enriched along the AP cell interfaces. Together, this suggests F-actin and myosin-II contribute to the contraction of cellular junctions and E-cadherin promotes new cellular

junctions, that is stabilized by Bazooka/PAR-3 (Zallen et al. 2004; Blankenship et al. 2006). It will be interesting to determine if these proteins are polarized during VNC assembly in *C. elegans* and if the loss of this polarity results in DD neuron spacing defects.

4.4 Future Directions: identifying downstream POP-1/TCF targets

Our findings showed that the canonical Wnt/β-catenin pathway is important for the regulation of cell intercalation during the formation of the VNC. We have shown that too little *bar-1* (in *bar-1* mutants) or too much *bar-1* (as in *pry-1* mutants) affects proper DD spacing via its interaction with POP-1/TCF. A comparison of transcriptomes between wild-type and *bar-1* mutants using microarray analysis identified nearly six thousand genes that were differentially expressed (Van Der Bent et al. 2014). This data set has the potential to shed insight into the downstream targets of POP-1/TCF required for proper DD neurons spacing. Two of these potential targets, the HOX and GATA transcription factors, are discussed below.

4.4.1 Hox gene targets

Wnt family proteins cooperate with conserved clusters of Hox genes to specify body patterning. The Hox cluster controls a variety of developmental processes including cell migration (Tihanyi et al. 2010), cell fate (Clark et al. 1993), and programmed cell death (Liu et al. 2006). In vertebrates, early Wnt signaling was shown to induce Hox expression profiles necessary to differentiate dorsal versus ventral motor neurons in the developing spinal cord (Nordström et al. 2006). In *C. elegans,* the Wnt protein *egl-20* regulates the HOX genes *mab-5*

(male abnormal), a component of the Hox cluster (*ceh-13, lin-39* and *mab-5, egl-5, ceh-23*). *mab-5* expression is required for neuronal migration in larval worms (Maloof et al. 1999). *mab-5* was recently shown to repress the transmembrane protein *mig-13*, which regulates actin accumulation in the leading edge of migrating cells. This regulation of the actin cytoskeleton helps direct anterior versus posterior neuronal migration (Wang et al. 2013). In the larval worm *lin-39* is expressed in the anterior most VNC neurons near DD1-DD2, whereas *mab-5* is expressed in neurons towards the tail (Kratsios et al. 2017). In the embryo, the Hox genes *ceh-13*, *lin-39*, and *mab-5* are expressed in the embryonic VNC around the same time Wnt/β-catenin-dependent DD neuron defects occur (Tihanyi et al. 2010; Brunschwig et al. 1999). In particular, recent work has shown that one of the Wnt transcription targets include *ceh-13* (Zacharias et al. 2015), and is a known regulator of cell migration (Tihanyi et al. 2010). It will be interesting to determine if canonical Wnt/β-catenin-dependent Hox expression regulates DD neuron spacing in the VNC.

Hox genes are also involved a variety of cell adhesion processes during morphogenesis. HOX proteins target transcriptional and signaling molecules called 'realizator genes.' In *Drosophila* the Hox gene *Abd-B* activates the genes *spalt*, *empty spiracle*, *cut*, and the ligand of the JAK/STAT pathway *unpaired*. The realizator molecules involved with these genes promote E-cadherin expression during the formation of the spiracle chamber. Interestingly, subsets of cells are differentially regulated by spiracle primary genes, which in turn generate an overlapping distribution of E-cadherin and non-classic cadherins (Lovegrove et al. 2006; Taniguchi 2014). In *Xenopus,* the HoxC6 gene can bind to the promoter of the neural cell adhesion molecule (N-CAM) (Jones et al. 1993). N-CAMs also affect cell motility and migration in cell culture (Guan et al. 2015). Although Hox genes are widely known to affect broad morphogenetic processes, it

is unclear whether they directly affect cell-intercalation. It is more likely that HOX genes, through one of their many 'realizator genes,' coordinate cell-cell intercalation by modifying cell adhesion or through the regulation of the actin cytoskeleton.

4.4.2 GATA transcription factors

GATA transcription factors contribute to a variety of developmental processes, but they are best characterized in regulatory switches that contribute to cell fate decisions. In *C. elegans* there are eleven GATA transcription factors each of which contribute to various cell differentiation and tissue specification processes: *elt-1*, *elt-2*, *elt-6*, and *elt-5* regulate epidermal specification; *med-1*, *med*-2, *end-1*, *end-3*, *elt-2* and *elt-7* guide intestinal differentiation; *elt-3* in epidermal development (summarized in (Block et al. 2015)). Recently, *elt-6*, *end-1*, and *end-3* have been shown to have POP-1/TCF binding sites (Zacharias et al. 2015). During embryogenesis, *elt-5* and *elt-6* exhibit robust expression in 'neurons and/or support cells' in the nervous system from as early as the comma stage through adulthood (Koh et al. 2001). While precise identity of these cells was not explored, it does raise the possibility that GATA mediated cell fusion or cell fate may be affecting DD neuron spacing in Wnt/β-catenin mutants. GATA proteins also regulate cell migration during embryonic convergent-extension. In *Xenopus* the transcription factors GATA5 and GATA6 are expressed in the leading edge of mesendoderm cells during CE-mediated gastrulation. Repression of GATA activity results in delayed gastrulation and a shortened AP body axis. In addition, reduced GATA activity also inhibitions cell migration in explants or dissociated cells (Fletcher et al. 2006; Weber et al. 2000). Similarly, in *C. elegans* the GATA gene *egl-18* is known to regulate HSN migration (Desai et al. 1988).

Together these studies show that GATA factors may be linked to different CE-mediated processes.

4.5 Conclusion and significance

In summary, we show that the canonical Wnt/β-catenin pathway is responsible for the polarization of a cell-neighbor exchange during VNC assembly in *C. elegans*. Proper intercalation during the cell-neighbor exchange was necessary to separate DD1 and DD2, and contributed to the spacing of these neurons along the AP axis. These findings are distinct from previous work in our laboratory showing that non-canonical PCP and *sax-3* pathways more broadly affect cell intercalation mechanisms by delaying rosette-resolution. These cell intercalation defects result in the anterior positioning of many DDs along the AP axis (Shah et al. 2017). Our findings demonstrate that many pathways cooperate to regulate distinct cellular intercalation leading to proper motor neuron spacing in the VNC of *C. elegans*.

PART 5: REFERENCES

Aman, A., & Piotrowski, T. 2010. Cell migration during morphogenesis. *Developmental Biology* 341(1): p.20–33. Available at: http://dx.doi.org/10.1016/j.ydbio.2009.11.014.

Bastock, R., & Strutt, D. 2007. The planar polarity pathway promotes coordinated cell migration during Drosophila oogenesis. *Development* 134(17): p.3055–3064. Available at: http://dev.biologists.org/cgi/doi/10.1242/dev.010447.

Van Der Bent, M.L. et al. 2014. Loss-of-function of β-catenin bar-1 slows development and activates the Wnt pathway in Caenorhabditis elegans. *Scientific Reports* 4: p.1–6.

Bertet, C., Suluk, L., & Lecuit, T. 2004. Myosin-dependent junction remodelling controls planar cell intercalation and axis elongation. *Nature* 429: p.667–671.

Bertrand, V. 2016. B-Catenin-Driven Binary Cell Fate Decisions in Animal Development. *Wiley Interdisciplinary Reviews: Developmental Biology* 5(3): p.377–388. Available at: https://www.ncbi.nlm.nih.gov/pmc/articles/PMC5069452/pdf/WDEV-5-377.pdf.

Blankenship, J.T., Backovic, S.T., Sanny, J.S.S.P., Weitz, O., & Zallen, J.A. 2006. Multicellular Rosette Formation Links Planar Cell Polarity to Tissue Morphogenesis. *Developmental Cell* 11(4): p.459–470.

Block, D.H., Shapira, M., Block, D.H.S., & Shapira, M. 2015. GATA transcription factors as tissue-specific master regulators for induced responses GATA transcription factors as tissue-speci fi c master regulators for induced responses. 4054(January 2016): p.1–5. Available at: https://www.ncbi.nlm.nih.gov/pmc/articles/PMC4826149/pdf/kwrm-04-04-1118607.pdf.

Brunschwig, K. et al. 1999. Anterior organization of the Caenorhabditis elegans embryo by the labial-like Hox gene ceh-13. *Development (Cambridge, England)* 126(7): p.1537–1546.

Carmona-Fontaine, C., Matthews, H., & Mayor, R. 2008. Directional cell migration in vivo: Wnt at the crest. *Cell adhesion & migration* 2(4): p.240–242. Available at: https://www.ncbi.nlm.nih.gov/pmc/articles/PMC2633683/pdf/cam0204_0240.pdf.

Clark, S.G., Chisholm, A.D., & Horvitz, H.R. 1993. Control of cell fates in the central body region of C. elegans by the homeobox gene lin-39. *Cell* 74(1): p.43–55. Available at: https://ac.els-cdn.com/009386749390293Y/1-s2.0-009386749390293Y-main.pdf?_tid=fee92aff-aa5f-4a1c-a301-5ef2d19ee834&acdnat=1527187217_390aa70da6af0929718b33a459484991.

Cong, F., & Varmus, H. 2004. Nuclear-cytoplasmic shuttling of Axin regulates subcellular localization of -catenin. *Proceedings of the National Academy of Sciences* 101(9): p.3882–3887. Available at: http://www.ncbi.nlm.nih.gov/pubmed/14981260%5Cnhttp://www.pubmedcentral.nih.gov/articlerender.fcgi?artid=PMC365714%5Cnhttp://www.pnas.org/cgi/doi/10.1073/pnas.0307344101.

Cormack BP, Valdivia RH, F.S. 1996. FACS-optimized mutants of the green fluorescent protein (GFP). *Gene* 173(1): p.33–38.

Curtin, J. et al. 2003. Mutation of Celsr1 disrupts planar polarity of inner ear hair cells and causes severe neural tube defects in the mouse. *Current Biology* 13(13): p.1129–33.

David I. Strutt, U.W.& M.M. 1997. The role of RhoA in tissue polarity and Frizzled signalling. *Nature* 387(May): p.292–5. Available at: https://www.nature.com/articles/387292a0.pdf.

Desai, C., Garriga, G., McIntire, S.L., & Horvitz, H.R. 1988. A genetic pathway for the development of the Caenorhabditis elegans HSN motor neuron. *Nature* 336(6200): p.638.

Devenport, D. 2016. Tissue morphodynamics: Translating planar polarity cues into polarized cell behaviors. *Seminars in Cell and Developmental Biology* 55: p.99–110.
Fagotto, F. 2013. Looking beyond the Wnt pathway for the deep nature of β-catenin. *EMBO Reports* 14(5): p.422–433.
Fletcher, A.G., Osterfield, M., Baker, R.E., & Shvartsman, S.Y. 2014. Vertex models of epithelial morphogenesis. *Biophysical Journal* 106(11): p.2291–2304. Available at: http://dx.doi.org/10.1016/j.bpj.2013.11.4498.
Fletcher, G., Jones, G.E., Patient, R., & Snape, A. 2006. A role for GATA factors in Xenopus gastrulation movements. *Mechanisms of Development* 123(10): p.730–745. Available at: https://ac.els-cdn.com/S092547730600102X/1-s2.0-S092547730600102X-main.pdf?_tid=8fcd38fd-dc39-44a8-a76e-0454a6254a9e&acdnat=1532386145_f61e9423c732d01eb5795baf6c080634.
Forrester, W.C., Kim, C., & Garriga, G. 2004. The Caenorhabditis elegans Ror RTK CAM-1 inhibits EGL-20/Wnt signaling in cell migration. *Genetics* 168(4): p.1951–1962. Available at: https://www.ncbi.nlm.nih.gov/pmc/articles/PMC1448710/pdf/1781.pdf.
Gleason, J.E., Szyleyko, E.A., & Eisenmann, D.M. 2006. Multiple redundant Wnt signaling components function in two processes during C. elegans vulval development. *Developmental Biology* 298(2): p.442–457. Available at: https://ac.els-cdn.com/S0012160606009754/1-s2.0-S0012160606009754-main.pdf?_tid=aa6795e4-2cdb-47cd-ba02-98338e39e262&acdnat=1527180832_e1fc581dd02bc5ca921f894083f5766f.
Goto, T., & Keller, R. 2002. The planar cell polarity gene Strabismus regulates convergence and extension and neural fold closure in Xenopus. *Developmental Biology* 247(1): p.165–181. Available at: https://ac.els-cdn.com/S0012160602906731/1-s2.0-S0012160602906731-main.pdf?_tid=ff3581dd-0188-4e88-9840-e408e62d2d82&acdnat=1538470607_5a3e41a775d1b903d90c4024d419df02.
Guan, F., Wang, X., & He, F. 2015. Promotion of cell migration by neural cell adhesion molecule (NCAM) is enhanced by PSA in a polysialyltransferase-specific manner. *PLoS ONE* 10(4): p.1–14.
Hall, D.H., Herndon, L.A., & Altun, Z. 2017. Introduction to C. elegans Embryo Anatomy. In *WormAtlas*,
Hardin, J., & King, R.S. 2013. The long and the short of Wnt signaling in C. elegans. *Journal of Chemical Information and Modeling* 53(9): p.1689–1699. Available at: https://www.ncbi.nlm.nih.gov/pmc/articles/PMC4523225/pdf/nihms710731.pdf.
Harris, J., Honigberg, L., Robinson, N., & Kenyon, C. 1996. Neuronal cell migration in C. elegans: regulation of Hox gene expression and cell position. *Development (Cambridge, England)* 122(10): p.3117–31. Available at: http://www.ncbi.nlm.nih.gov/pubmed/8898225%5Cnhttp://dev.biologists.org.proxy.library.uu.nl/content/122/10/3117.short.
Hartenstein, V., Technau, G.M., & Campos-Ortega, J.A. 1985. Fate-mapping in wild-typeDrosophila melanogaster. *Wilhelm Roux's Archives of Developmental Biology* 194(4): p.213–216. Available at: http://link.springer.com/10.1007/BF00848248.
Harterink, M. et al. 2011. Neuroblast migration along the anteroposterior axis of C. elegans is controlled by opposing gradients of Wnts and a secreted Frizzled-related protein. *Development* 138(14): p.2915–2924. Available at: http://dev.biologists.org/cgi/doi/10.1242/dev.064733.
Henderson, B.R. 2000. Nuclear-cytoplasmic shuttling of APC regulates β-catenin subcellular

localization and turnover. *Nature Cell Biology* 2(9): p.653–60.
Henderson, B.R., & Fagotto, F. 2002. The ins and outs of APC and beta-catenin nuclear transport. *EMBO reports* 3(9): p.834–9. Available at: http://embor.embopress.org/content/3/9/834.abstract.
Hobert, O. 2002. PCR fusion-based approach to create reporter Gene constructs for expression analysis in transgenic C. elegans. *BioTechniques* 32(4): p.738–730. Available at: http://hobertlab.org/wp-content/uploads/2013/01/PCR_Fusion.pdf.
Hoppler, S., & Kavanagh, C.L. 2007. Wnt signalling: variety at the core. *Journal of Cell Science* 120(3): p.385–393. Available at: http://jcs.biologists.org/cgi/doi/10.1242/jcs.03363.
Huang, S., Shetty, P., Robertson, S.M., & Lin, R. 2007. Binary cell fate specification during C. elegans embryogenesis driven by reiterated reciprocal asymmetry of TCF POP-1 and its coactivator -catenin SYS-1. *Development* 134(14): p.2685–2695. Available at: http://dev.biologists.org/cgi/doi/10.1242/dev.008268.
Jackson, B.M., & Eisenmann, D.M. 2012. beta-catenin-dependent Wnt signaling in C. elegans: teaching an old dog a new trick. *Cold Spring Harb Perspect Biol* 4(8): p.a007948. Available at: http://www.ncbi.nlm.nih.gov/pubmed/22745386%5Cnhttp://www.ncbi.nlm.nih.gov/pmc/articles/PMC3405868/pdf/cshperspect-WNT-a007948.pdf.
Janssen, R. et al. 2010. Conservation, loss, and redeployment of Wnt ligands in protostomes: Implications for understanding the evolution of segment formation. *BMC Evolutionary Biology* 10(1): p.1–21. Available at: https://bmcevolbiol.biomedcentral.com/track/pdf/10.1186/1471-2148-10-374.
Jenny, A., Reynolds-Kenneally, J., Das, G., Burnett, M., & Mlodzik, M. 2005. Diego and Prickle regulate frizzled planar cell polarity signalling by competing for Dishevelled binding. *Nature Cell Biology* 7(7): p.691–697. Available at: https://www.nature.com/articles/ncb1271.pdf.
Jones, F.S., Holst, B.D., Minowa, O., De Robertis, E.M., & Edelman, G.M. 1993. Binding and transcriptional activation of the promoter for the neural cell adhesion molecule by HoxC6 (Hox-3.3). *Proc.Natl.Acad.Sci.U.S.A* 90(14): p.6557–6561. Available at: http://www.pnas.org/content/pnas/90/14/6557.full.pdf.
Josephson, M.P., Chai, Y., Ou, G., & Lundquist, E.A. 2016. EGL-20/Wnt and MAB-5/Hox act sequentially to inhibit anterior migration of neuroblasts in C. Elegans. *PLoS ONE* 11(2): p.1–20. Available at: https://www.ncbi.nlm.nih.gov/pmc/articles/PMC4749177/pdf/pone.0148658.pdf.
Kim, C., & Forrester, W.C. 2003. Functional analysis of the domains of the C. elegans Ror receptor tyrosine kinase CAM-1. *Developmental Biology* 264(2): p.376–390. Available at: https://ac.els-cdn.com/S0012160603005293/1-s2.0-S0012160603005293-main.pdf?_tid=96d3113b-fdd6-4989-8cba-1400fcaa69fb&acdnat=1538143891_8b1b506d14758f01ed5ea9c599488227.
Koh, K., & Rothman, J.H. 2001. ELT-5 and ELT-6 are required continuously to regulate epidermal seam cell differentiation and cell fusion in C. elegans. *Development (Cambridge, England)* 138: p.3867–3880. Available at: http://dev.biologists.org/content/develop/138/15/3867.full.pdf.
Koleske, A.J. et al. 1998. Essential roles for the Abl and Arg tyrosine kinases in neurulation. *Neuron* 21(6): p.1259–1272. Available at: https://ac.els-cdn.com/S0896627300806467/1-s2.0-S0896627300806467-main.pdf?_tid=41f6749a-58c7-4b1f-855c-

7dd172ebf5c4&acdnat=1530799506_1cdaa5a8b531382d73e3532334a51812.
Korswagen, H.C. et al. 2002. The Axin-like protein PRY-1 is a negative regulator of a canonical The Axin-like protein PRY-1 is a negative regulator of a canonical Wnt pathway in C . elegans. : p.1291–1302. Available at: https://www.ncbi.nlm.nih.gov/pmc/articles/PMC186271/pdf/X10.pdf.
Kratsios, P. et al. 2017. An intersectional gene regulatory strategy defines subclass diversity of C. Elegans motor neurons. *eLife* 6: p.1–31. Available at: https://www.ncbi.nlm.nih.gov/pmc/articles/PMC5498135/pdf/elife-25751.pdf.
Kühl, M. et al. 2001. Antagonistic regulation of convergent extension movements in Xenopus by Wnt/β-catenin and Wnt/Ca2+ signaling. *Mechanisms of Development* 106(1–2): p.61–76. Available at: https://ac.els-cdn.com/S0925477301004166/1-s2.0-S0925477301004166-main.pdf?_tid=b105ff94-d51b-4ff4-98ec-029d325ce8f7&acdnat=1538387087_3e07cfd3d870f9c2e1cd82774589e709.
Lecuit, T., & Yap, A.S. 2015. E-cadherin junctions as active mechanical integrators in tissue dynamics. *Nature Cell Biology* 17(5): p.533–539. Available at: http://dx.doi.org/10.1038/ncb3136.
Lin, R., Hill, R.J., & Priess, J.R. 1998. POP-1 and anterior-posterior fate decisions in C. elegans embryos. *Cell* 92(2): p.229–239. Available at: https://ac.els-cdn.com/S0092867400809174/1-s2.0-S0092867400809174-main.pdf?_tid=e0bed211-681d-431e-b78e-48b6d1fac3cd&acdnat=1525192217_5a6e2d032669f8bfcca2c9cc4bf194d0.
Liu, H., Strauss, T., Potts, M., & Cameron, S. 2006. Direct regulation of egl-1 and of programmed cell death by the Hox protein MAB-5 and by CEH-20, a C. elegans homolog of Pbx1. *Development* 133(4): p.641–650. Available at: http://dev.biologists.org/cgi/doi/10.1242/dev.02234.
Liu, J., Phillips, B.T., Amaya, M.F., Kimble, J., & Xu, W. 2008. The C. elegans SYS-1 Protein Is a Bona Fide β-Catenin. *Developmental Cell* 14(5): p.751–761. Available at: https://www.ncbi.nlm.nih.gov/pmc/articles/PMC2538363/pdf/nihms48743.pdf.
Lo, M.C., Gay, F., Odom, R., Shi, Y., & Lin, R. 2004. Phosphorylation by the β-catenin/MAPK complex promotes 14-3-3-mediated nuclear export of TCF/POP-1 in signal-responsive cells in C. elegans. *Cell* 117(1): p.95–106. Available at: https://www.cell.com/cell/pdf/S0092-8674(04)00203-X.pdf.
Lovegrove, B. et al. 2006. Coordinated Control of Cell Adhesion, Polarity, and Cytoskeleton Underlies Hox-Induced Organogenesis in Drosophila. *Current Biology* 16(22): p.2206–2216. Available at: https://ac.els-cdn.com/S0960982206022226/1-s2.0-S0960982206022226-main.pdf?_tid=6f107396-2f60-4e7b-8e48-279fc2b5a3d3&acdnat=1532441833_299eddc3e612a7e7d43e7c0711043df4.
Maloof, J.N., Whangbo, J., Harris, J.M., Jongeward, G.D., & Kenyon, C. 1999. A Wnt signaling pathway controls Hox gene expression and neuroblast migration in C . elegans. 49: p.37–49. Available at: http://dev.biologists.org/content/develop/126/1/37.full.pdf.
Markiewicz, E. et al. 2006. The inner nuclear membrane protein Emerin regulates β-catenin activity by restricting its accumulation in the nucleus. *EMBO Journal* 25(14): p.3275–3385. Available at: https://www.ncbi.nlm.nih.gov/pmc/articles/PMC1523183/pdf/7601230a.pdf.
Maro, G.S., Klassen, M.P., & Shen, K. 2009. A β-catenin-dependent Wnt pathway mediates anteroposterior axon guidance in C. elegans motor neurons. *PLoS ONE* 4(3). Available at: http://journals.plos.org/plosone/article/file?id=10.1371/journal.pone.0004690&type=printable.

Maung, S.M.T.W., & Jenny, A. 2011. Planar cell polarity in Drosophila. *Organogenesis* 7(3): p.165–179. Available at: http://www.tandfonline.com/doi/abs/10.4161/org.7.3.18143.
McCrea, P.D., & Gu, D. 2010. The catenin family at a glance. *Journal of Cell Science* 123(5): p.637–642. Available at: http://jcs.biologists.org/cgi/doi/10.1242/jcs.039842.
Mege, R., & Ishiyama, N. 2017. Integration of Cadherin Adhesion and Cytoskeleton at Adherens Junctions. *Cold Spring Harb Perspect Biol.* 9(5): p.pii: a038738.
Modzelewska, K. et al. 2013. Neurons Refine the Caenorhabditis elegans Body Plan by Directing Axial Patterning by Wnts. *PLoS Biology* 11(1): p.1–22. Available at: http://journals.plos.org/plosbiology/article/file?id=10.1371/journal.pbio.1001465&type=printable.
Murgan, S., & Bertrand, V. 2015. How targets select activation or repression in response to Wnt. *Worm* 4(4): p.e1086869.
Myers, T.R., & Greenwald, I. 2007. Wnt signal from multiple tissues and lin-3/EGF signal from the gonad maintain vulval precursor cell competence in Caenorhabditis elegans. *Proceedings of the National Academy of Sciences of the United States of America* 104(51): p.20368–73. Available at: http://www.pnas.org/cgi/content/long/104/51/20368.
Natarajan, L., Jackson, B.M., Szyleyko, E., & Eisenmann, D.M. 2004. Identification of evolutionarily conserved promoter elements and amino acids required for function of the C. elegans β-catenin homolog BAR-1. *Developmental Biology* 272(2): p.536–557.
Nishimura, T., Honda, H., & Takeichi, M. 2012. Planar cell polarity links axes of spatial dynamics in neural-tube closure. *Cell* 149(5): p.1084–1097.
Nordström, U., Maier, E., Jessell, T.M., & Edlund, T. 2006. An early role for Wnt signaling in specifying neural patterns of Cdx and Hox gene expression and motor neuron subtype identity. *PLoS Biology* 4(8): p.1438–1452. Available at: http://journals.plos.org/plosbiology/article/file?id=10.1371/journal.pbio.0040252&type=printable.
Pan, C.L. et al. 2006. Multiple Wnts and Frizzled receptors regulate anteriorly directed cell and growth cone migrations in Caenorhabditis elegans. *Developmental Cell* 10(3): p.367–377. Available at: https://ac.els-cdn.com/S1534580706000748/1-s2.0-S1534580706000748-main.pdf?_tid=14b0954d-24f5-43c4-94ad-6cea651aac84&acdnat=1538140556_9e1fc8c80dc09933dd72747ae79da04a.
Park, T.J., Haigo, S.L., & Wallingford, J.B. 2006. Ciliogenesis defects in embryos lacking inturned or fuzzy function are associated with failure of planar cell polarity and Hedgehog signaling. *Nature Genetics* 38(3): p.303–311.
Reynolds, A. et al. 2007. Mutations in VANGL1 Associated with Neural-Tube Defects. *The New England Journal of Medicine* 356(14): p.1432–1437. Available at: https://www.nejm.org/doi/pdf/10.1056/NEJMoa060651.
Rieckher, M., & Tavernarakis, N. 2017. Generation of Caenorhabditis elegans Transgenic Animals by DNA Microinjection. *Bio-Protocol* 7(19). Available at: http://www.bio-protocol.org/e2565.
Rigo-Watermeier, T. et al. 2012. Functional conservation of Nematostella Wnts in canonical and noncanonical Wnt-signaling. *Biology Open* 1(1): p.43–51. Available at: http://bio.biologists.org/cgi/doi/10.1242/bio.2011021.
Sai, X., Yonemura, S., & Ladher, R.K. 2014. Junctionally restricted RhoA activity is necessary for apical constriction during phase 2 inner ear placode invagination. *Developmental Biology* 394(2): p.206–216. Available at: http://dx.doi.org/10.1016/j.ydbio.2014.08.022.

Sawa H., K.H.C. 2013. Wnt signaling in C. elegans. In I. Greenwald (ed) *Wormbook*, Available at: http://www.wormbook.org.

Schambony A, W.D. 2003. Madame Curie Bioscience Database [Internet]. In *[Internet]*, Austin (TX): Landes Bioscience

Shah, P.K., Tanner, M.R., Kovacevic, I., Perkins, T.J., & Bao, Z. 2017. PCP and SAX-3 / Robo Pathways Cooperate to Regulate Convergent Extension-Based Nerve Cord Short Article PCP and SAX-3 / Robo Pathways Cooperate to Regulate Convergent Extension-Based Nerve Cord Assembly in C . elegans. *Developmental Cell* 41(2): p.195–203.e3. Available at: http://dx.doi.org/10.1016/j.devcel.2017.03.024.

Siegfried, K.R., Kidd, A.R., Chesney, M.A., & Kimble, J. 2004. The sys-1 and sys-3 Genes Cooperate with Wnt Signaling to Establish the Proximal-Distal Axis of the Caenorhabditis elegans Gonad. *Genetics* 166(1): p.171–186. Available at: https://www.ncbi.nlm.nih.gov/pmc/articles/PMC1470708/pdf/15020416.pdf.

Siegfried, K.R., & Kimble, J. 2002. POP-1 controls axis formation during early gonadogenesis in C. elegans. *Development (Cambridge, England)* 129: p.443–453. Available at: http://dev.biologists.org/content/develop/129/2/443.full.pdf.

Silhankova, M., & Korswagen, H.C. 2007. Migration of neuronal cells along the anterior-posterior body axis of C. elegans: Wnts are in control. *Current Opinion in Genetics and Development* 17(4): p.320–325.

Soto, M.C. 2017. Sequential Rosettes Drive C. elegans Ventral Nerve Cord Assembly. *Developmental Cell* 41(2): p.121–122.

Tahinci, E. et al. 2007. Lrp6 is required for convergent extension during Xenopus gastrulation. *Development* 134(22): p.4095–4106.

Tamada, M., Farell, D.L., & Zallen, J.A. 2012. Abl regulates planar polarized junctional dynamics through βcatenin tyrosine phosphorylation. *Developmental Cell* 22(2): p.309–319.

Tamai, K. et al. 2004. A Mechanism for Wnt Coreceptor Activation. *Molecular Cell* 13(1): p.149–156. Available at: https://ac.els-cdn.com/S1097276503004842/1-s2.0-S1097276503004842-main.pdf?_tid=616c8446-b23e-4ce7-84d5-419b4401305b&acdnat=1532368296_a1bdb529e44d31e15845bfb7ecf543a7.

Taniguchi, Y. 2014. Hox transcription factors: Modulators of cell-cell and cell-extracellular matrix adhesion. *BioMed Research International* 2014. Available at: https://www.ncbi.nlm.nih.gov/pmc/articles/PMC4127299/pdf/BMRI2014-591374.pdf.

Thorpe, C.J., Schlesinger, A., Clayton Carter, J., & Bowerman, B. 1997. Wnt signaling polarizes an early C. elegans blastomere to distinguish endoderm from mesoderm. *Cell* 90(4): p.695–705. Available at: https://ac.els-cdn.com/S0092867400805309/1-s2.0-S0092867400805309-main.pdf?_tid=c49c8f9c-f395-4b9c-8bfb-94b6039086e1&acdnat=1531844616_efdfbe4b4b0d65217f60d77fddf2e8a6.

Tihanyi, B. et al. 2010. The C. elegans Hox gene ceh-13 regulates cell migration and fusion in a non-colinear way. Implications for the early evolution of Hox clusters. *BMC Developmental Biology* 10. Available at: https://bmcdevbiol.biomedcentral.com/track/pdf/10.1186/1471-213X-10-78.

Torpe, N., & Pocock, R. 2014. Regulation of Axonal Midline Guidance by Prolyl 4-Hydroxylation in *Caenorhabditis elegans*. *The Journal of Neuroscience* 34(49): p.16348–16357. Available at: http://www.jneurosci.org/lookup/doi/10.1523/JNEUROSCI.1322-14.2014.

Trichas, G. et al. 2012. Multi-cellular rosettes in the mouse visceral endoderm facilitate the

ordered migration of anterior visceral endoderm cells. *PLoS Biology* 10(2).
Tsuboi, D., Hikita, T., Qadota, H., Amano, M., & Kaibuchi, K. 2005. Regulatory machinery of UNC-33 Ce-CRMP localization inneurites during neuronal development in Caenorhabditis elegans. *J Neurochem* 95(6): p.1629–1641.
Wallingford, J.B. et al. 2000. Dishevelled controls cell polarity during Xenopus gastrulation. *Nature* 405(6782): p.81–85. Available at: https://www.nature.com/articles/35011077.pdf.
Wallingford, J.B. 2006. Planar cell polarity, ciliogenesis and neural tube defects. *Human Molecular Genetics* 15(SUPPL. 2): p.227–234.
Wallingford, J.B., Fraser, S.E., & Harland, R.M. 2002. Convergent ExtensionThe Molecular Control of Polarized Cell Movement during Embryonic Development. *Developmental Cell* 2(6): p.695–706.
Wallingford, J.B., Vogeli, K.M., & Harland, R.M. 2001. Regulation of convergent extension in Xenopus by Wnt5a and Frizzled-8 is independent of the canonical Wnt pathway. *International Journal of Developmental Biology* 45(1): p.225–227.
Walston, T.D., & Hardin, J. 2006. Wnt-dependent spindle polarization in the early C. elegans embryo. *Seminars in Cell and Developmental Biology* 17(2): p.204–213. Available at: https://ac.els-cdn.com/S1084952106000413/1-s2.0-S1084952106000413-main.pdf?_tid=5e31a153-a032-4570-bcb5-5d1b6c603c91&acdnat=1538307408_15c3714b999257dabf9589bccab3aaeb.
Wang, L., Liu, X., Gusev, E., Wang, C., & Fagotto, F. 2014. Regulation of the phosphorylation and nuclear import and export of -catenin by APC and its cancer-related truncated form. *Journal of Cell Science* 127(8): p.1647–1659. Available at: http://jcs.biologists.org/cgi/doi/10.1242/jcs.131045.
Wang, X. et al. 2013. Transmembrane protein MIG-13 links the Wnt signaling and Hox genes to the cell polarity in neuronal migration. *Proceedings of the National Academy of Sciences* 110(27): p.11175–11180. Available at: http://www.pnas.org/cgi/doi/10.1073/pnas.1301849110.
Weber, H., Symes, C.E., Walmsley, M.E., Rodaway, A.R., & Patient, R.K. 2000. A role for GATA5 in Xenopus endoderm specification. *Development (Cambridge, England)* 127(20): p.4345–60. Available at: http://www.ncbi.nlm.nih.gov/pubmed/11003835.
Weidinger, G., & Moon, R.T. 2003. When Wnts antagonize Wnts. *Journal of Cell Biology* 162(5): p.753–755. Available at: https://www.ncbi.nlm.nih.gov/pmc/articles/PMC2173824/pdf/200307181.pdf.
Westfall, T.A. et al. 2003. Wnt-5/pipetail functions in vertebrate axis formation as a negative regulator of Wnt/β-catenin activity. *Journal of Cell Biology* 162(5): p.889–898. Available at: https://www.ncbi.nlm.nih.gov/pmc/articles/PMC2173822/pdf/200303107.pdf.
Whangbo, J., & Kenyon, C. 1999. A Wnt signaling system that specifies two patterns of cell migration in C. elegans. *Molecular Cell* 4(5): p.851–858. Available at: https://www.cell.com/molecular-cell/pdf/S1097-2765(00)80394-9.pdf.
Wiechens, N., & Fagotto, F. 2001. CRM1- and Ran-independent nuclear export of β-catenin. *Current Biology* 11(1): p.18–27. Available at: https://www.cell.com/current-biology/pdf/S0960-9822(00)00045-2.pdf.
Wodarz, A., & Nusse, R. 1998. Mechanisms of Wnt Signaling in Development. *Annu. Rev. Cell Dev. Biol* 14: p.59–88.
Yang, X.-D. et al. 2011. Distinct and mutually inhibitory binding by two divergent -catenins coordinates TCF levels and activity in C. elegans. *Development* 138(19): p.4255–4265.

Available at: http://dev.biologists.org/cgi/doi/10.1242/dev.069054.
Yanshu Wang, Nino Guo, J.N. 2006. The Role of Frizzled3 and Frizzled6 in Neural Tube Closure and in the Planar Polarity of Inner-Ear Sensory Hair Cells. *The Journal of Neuroscience* 26(8): p.2147–2156.
Ye, Z. et al. 2013. Wnt5a uses CD146 as a receptor to regulate cell motility and convergent extension. *Nature Communications* 4. Available at: https://www.nature.com/articles/ncomms3803.pdf.
Zacharias, A.L., Walton, T., Preston, E., & Murray, J.I. 2015. Quantitative Differences in Nuclear β-catenin and TCF Pattern Embryonic Cells in C. elegans. *PLoS Genetics* 11(10). Available at: http://journals.plos.org/plosgenetics/article/file?id=10.1371/journal.pgen.1005585&type=printable.
Zallen, J.A., & Wieschaus, E. 2004. Patterned gene expression directs bipolar planar polarity in Drosophila. *Developmental Cell* 6(3): p.343–355. Available at: https://ac.els-cdn.com/S1534580704000607/1-s2.0-S1534580704000607-main.pdf?_tid=00785d50-0bd9-4af3-b29d-c4870aef18eb&acdnat=1530727912_ca065f05cae371b1e59c4b4174fdbef1.
Zecca, M., Basler, K., & Struhl, G. 1996. Direct and long-range action of a wingless morphogen gradient. *Cell* 87(5): p.833–844. Available at: https://ac.els-cdn.com/S0092867400819911/1-s2.0-S0092867400819911-main.pdf?_tid=0d153a81-6c11-4349-89ad-5d484e816b71&acdnat=1527182268_44630fe072f90194d3b214158ff215dd.
Zhang, L. et al. 2016. A lateral signalling pathway coordinates shape volatility during cell migration. *Nature Communications* 7(May): p.1–13. Available at: http://dx.doi.org/10.1038/ncomms11714.
Zinovyeva, A.Y., Yamamoto, Y., Sawa, H., & Forrester, W.C. 2008. Complex network of Wnt signaling regulates neuronal migrations during Caenorhabditis elegans development. *Genetics* 179(3): p.1357–1371. Available at: https://www.ncbi.nlm.nih.gov/pmc/articles/PMC2475739/pdf/GEN17931357.pdf.

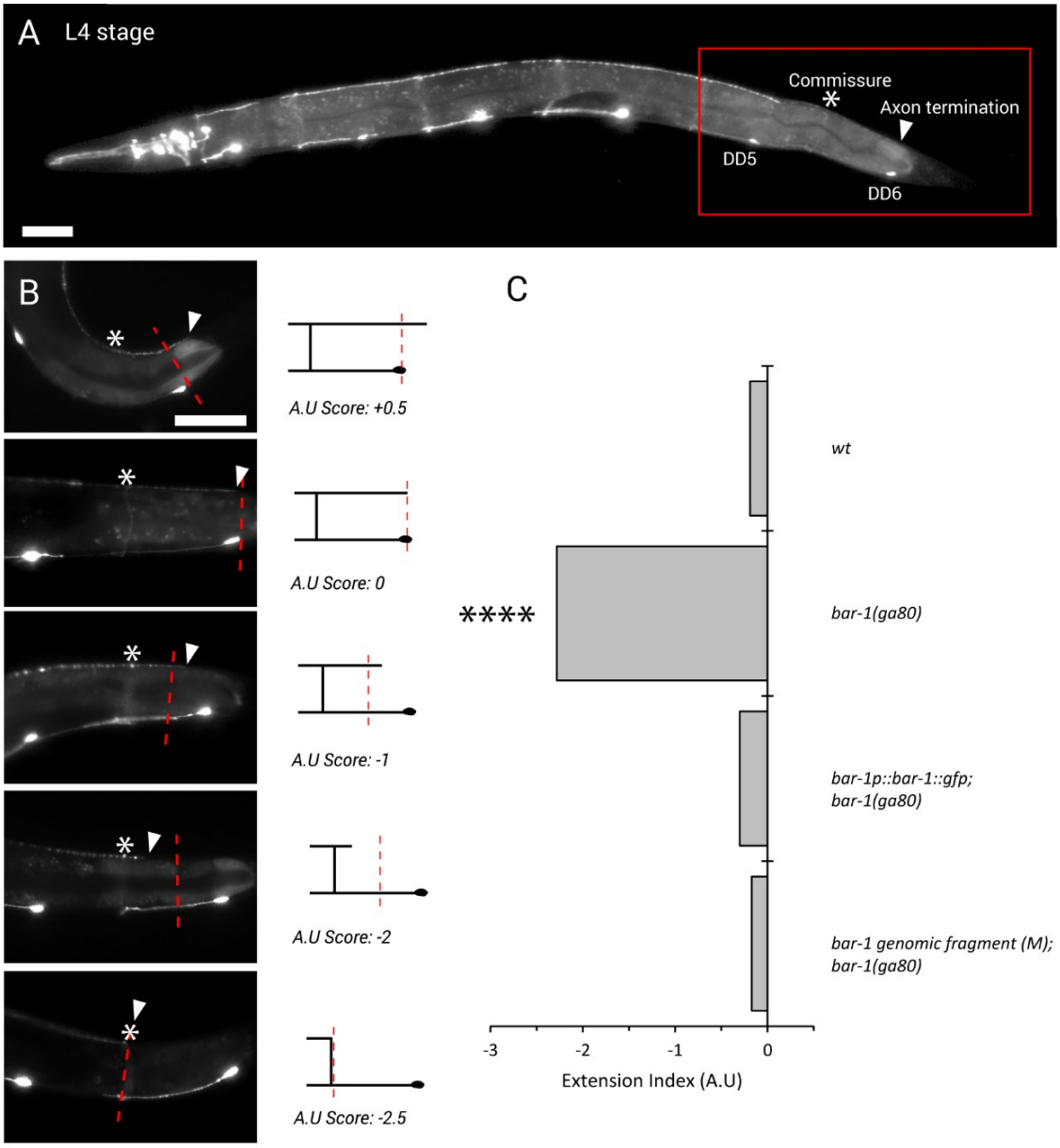

Appendix Figure 1. DD6 axon guidance defects in *bar-1* mutants
(A) A wild-type L4 stage larval worm. DD6 terminates its dorsal axonal process at the same anterior-posterior position as its cell body. Arrow indicates the DD6 axonal termination point. Asterisk indicates DD6 commissure (B) A set of representative axon termination phenotypes. An arbitrary score was given for each class: +0.5 for overextension, 0 for *wt* or equal termination, -1 for underextension greater than half-way between the commissure and DD6 cell body, -2 for underextension less than half-way, and -2.5 for underextension which terminates at the dorsal commissure. (C) The transcriptional *bar-1* genomic PCR fragment (M) and the BAR-1::GFP translational fusion (zyEx80) rescues of the *bar-1(ga80)* axonal underextension phenotype. Significance: $p < 0.0001$ (****) using chi-squared tests.

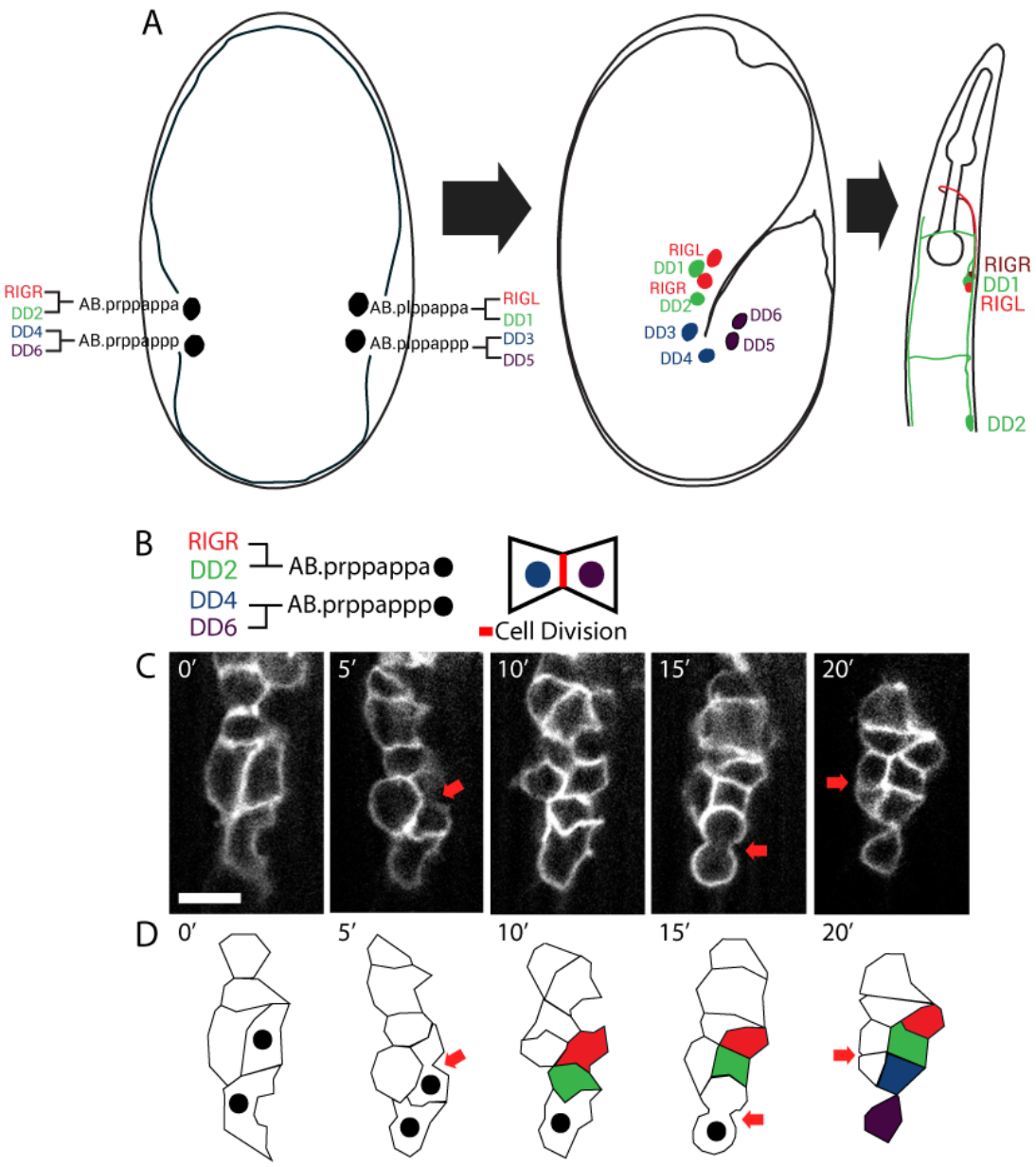

Appendix Figure 2. DD and RIG lineages during development
(A) A schematic showing the neuroblast position of the DD and RIG parental lineages AB.prppappa (RIGR, DD2) and AB.prppappp (DD4, DD6) on the left and AB.plppappa (RIGL, DD1) and AB.plppappp (DD3, DD5) on the right. After being born, the DD and RIGs move towards the ventral midline of the embryo (bean stage) and undergo cell intercalations along the anterior-to-posterior axis (1.5-fold stage), which persist through adulthood (L4 worm). (B) A key where parental lineages (black dot) result in a color-coded neuron. Cell division of parental lineage is indicated in red (arrow). (C) In the embryo, a membrane bound mCherry driven by a *cnd-1* promotor labels, amongst other cells, the AB.prppappa and AB.prppappp lineages. (D) The cell division of the AB.prppappa and AB.prppappp lineages (black dots) leading to RIG and DD neurons. Red arrows indicate cell divisions. Time represents (+) minutes relative to first image. Scale bar is 10 μm.

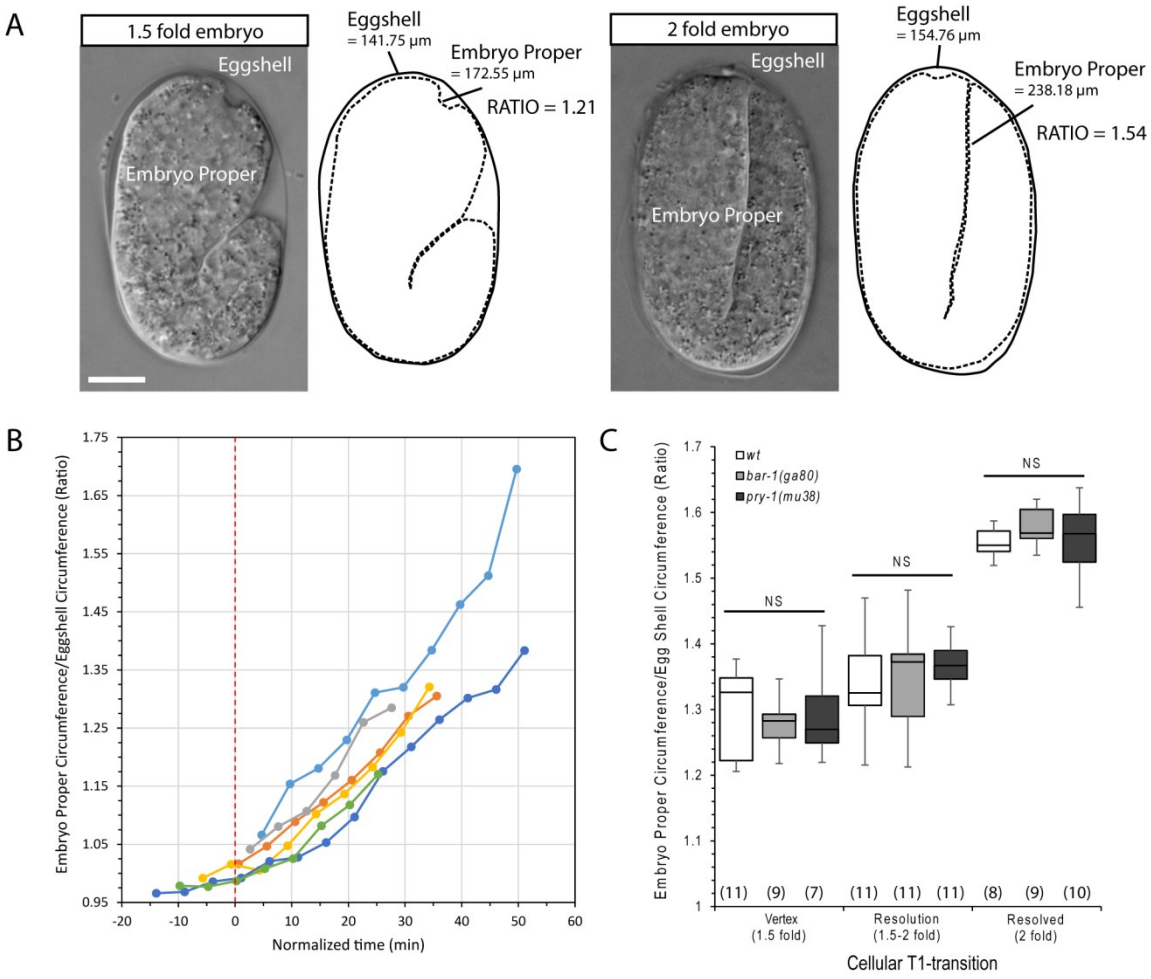

Appendix Figure 3. Calculations to determine embryonic developmental stage
(A) Representative 1.5- and 2-fold embryos. A ratio between the circumference of the embryo's outermost layer (eggshell) to inner embryo (termed embryo proper) was used to determine 'developmental stage' during embryogenesis. Scale bar is 10 µm. (B) The ratio of each embryo (assigned separate colors) increase linearly from the bean to 2-fold stages (n = 6). Time (0 min) is at the bean stage where eggshell circumference is equal embryo proper circumference (ratio = 1.0). (D) Developmental timing, as a function of embryo size, of the cell neighbor exchange (T1 transitions) between DD1, DD2, RIGL and DA2 neurons, is not affected in mutant backgrounds. Significance tested using two-tailed t-tests.